Fish and Shellfish Immunology 95 (2019) 368–382

Contents lists available at ScienceDirect

Fish and Shellfish Immunology

journal homepage: www.elsevier.com/locate/fsi

Full length article

Exploration of the influence of surface proteins on the probiotic activity of *Lactobacillus pentosus* HC-2 in the *Litopenaeus vannamei* midgut via label-free quantitative proteomic analysis

Yang Du[a,b], Han Fang[b,c], Xuqing Shao[f], Mei Liu[a,b], Keyong Jiang[a,b], Mengqiang Wang[a,b], Baojie Wang[a,b,*], Lei Wang[a,b,d,**]

[a] CAS Key Laboratory of Experimental Marine Biology, Institute of Oceanology, Chinese Academy of Sciences, 7 Nanhai Road, Qingdao, 266071, China
[b] Laboratory for Marine Biology and Biotechnology, Qingdao National Laboratory for Marine Science and Technology, Qingdao, 266237, China
[c] University of Chinese Academy of Sciences, 19 Yuquan Road, Beijing, 100049, China
[d] CAS Center for Ocean Mega-Science, Chinese Academy of Sciences, Qingdao, 266400, China
[f] Shandong Cigna Detection Technology Co., Ltd, Qingdao, 266237, China

ARTICLE INFO

Keywords:
Litopenaeus vannamei
Lactobacillus pentosus HC-2
Surface proteins
Proteomic analysis

ABSTRACT

Our previous work showed that using *Lactobacillus pentosus* HC-2 as a probiotic could improve the growth performance, immune response, gut bacterial diversity and disease resistance of *Litopenaeus vannamei*. However, the probiotic mechanism had not been fully characterized. In the present study, histology and proteomic analysis were performed to explore the influence of HC-2 surface protein on its probiotic effects on *L. vannamei* after feeding either the intact surface proteins, the probiotic treated with lithium chloride (LiCl) to remove noncovalently bound surface proteins or no probiotic for four weeks. Histological observation found that feeding with normal HC-2 obviously improved the intestinal histology and enhanced the protective effect against pathogen damage, but feeding with LiCl-treated HC-2 did not improve the intestinal environment. A total of over 2764 peptides and 1118 uniproteins were identified from the *L. vannamei* midgut; 211 proteins were significantly differentially expressed in the normal HC-2 group compared with the control group; 510 proteins were significantly differentially expressed in the LiCl-treated HC-2 group compared with the control group, and 458 proteins were significantly differentially expressed in the LiCl-treated HC-2 group compared with the normal HC-2 group. GO/KEGG enrichment analysis of the significantly different proteins demonstrated that feeding normal HC-2 mainly induced immune response, metabolic, cell adhesion and cell-cell signaling-related protein upregulation, which contributed to bacterial adhesion and colonization in the midgut to improve the shrimp immune system and growth, but these proteins were suppressed after the shrimp were fed bacteria deprived of surface proteins. Taken together, these results indicate that the surface proteins were indispensable for HC-2 to execute probiotic effects in the shrimp midgut.

1. Introduction

Litopenaeus vannamei is one of the most valuable crustacean aquaculture species worldwide because of its high nutrition value and tolerance to extensive salinity [1]. However, water environment deterioration, frequent disease outbreaks caused by viruses, such as WSSV, YHV and IHHNV, or by bacteria, such as the genus *Vibrio,* are more prominent issues that result from the rapidly growing shrimp aquaculture industry [2,3]. Thus, there is international concern about managing the tough problem by supplying probiotic bacterial cells in food or in the aquatic environment to control the infectious diseases by strengthening the bodies of aquatic animals [4,5]. Among the available probiotics, lactic acid bacteria (LAB) are commonly used and recommended, including such species as *Lactobacillus pentosus, Lactobacillus helveticus, Lactobacillus delbrueckii, Lactobacillus acidophilus* and *Lactobacillus plantarum,* which have been widely administered to

* Corresponding author. CAS Key Laboratory of Experimental Marine Biology, Institute of Oceanology, Chinese Academy of Sciences, 7 Nanhai Road, Qingdao, 266071, China.
** Corresponding author. CAS Key Laboratory of Experimental Marine Biology, Institute of Oceanology, Chinese Academy of Sciences, 7 Nanhai Road, Qingdao, 266071, China.
E-mail addresses: wangbaojie@qdio.ac.cn (B. Wang), wanglei@qdio.ac.cn (L. Wang).

https://doi.org/10.1016/j.fsi.2019.10.059
Received 30 April 2019; Received in revised form 11 October 2019; Accepted 28 October 2019
Available online 01 November 2019

significantly improve host immune status, strengthen host digestion, modulate the bacterial community, and antagonize opportunistic pathogens [6–8].

The mechanisms of LAB probiotic functionality are not completely understood, but it is hypothesized that the maximum probiotic effects can be achieved if the organisms adhere to mucus and/or intestinal epithelial cells [9]. It has recently been suggested that surface proteins of lactobacilli participate in the adhesion to epithelial cell lines, gastrointestinal mucins, or extracellular matrix proteins [10–12]. Indeed, except for mediating binding ability, surface proteins are also involved in maintaining the shape of the bacteria, functioning as molecular sieves, providing immunomodulation and extracellular enzyme binding sites to the host [13–15]. Because these proteins bind to the outermost layer of the bacteria with noncovalent bonds, they enable the use of denaturants, such as lithium chloride (LiCl), guanidine hydrochloride (GuHCl), urea or metal chelating agents, which depolymerize them to monomers [16–18].

In our previous work, we isolated a *Lactobacillus pentosus* HC-2 strain that provides high antimicrobial activity against *Vibrio* pathogens and adhesive ability to intestinal mucosa, regulates intestinal flora, and enhances growth performance, immune responses, and disease resistance after feeding to *L. vannamei* [19–21]. The present study aimed to further investigate the mediating function of *L. pentosus* HC-2 surface proteins in the process of colonization and immune regulation of HC-2 to *L. vannamei*. Label-free proteomic analysis was applied to characterize the protein expression induced by surface proteins in the midgut of shrimp fed LiCl-treated HC-2.

2. Materials and methods

2.1. Bacterial growth and surface protein shaving

Lactobacillus pentosus HC-2 (GenBank Accession No. KU995298) was previously isolated from the intestinal tract of fish (*Acanthogobius hasta*) by our laboratory [21] and were stored at −80 °C in de Man, Rogosa, and Sharpe (MRS) broth containing 20% (v/v) glycerol. After recovery, the bacteria were cultured unstirred in MRS medium at 37 °C under anaerobic conditions.

Cell surface protein shaving was performed as previously described [22]. Briefly, a 500 mL culture of bacteria on the transition between late exponential and stationary phase ($OD_{600} \approx 1.7$) were harvested by centrifugation (3000 × *g*, 10 min, 4 °C). Then, the cell pellets were washed three times with 1 M phosphate-buffered saline (PBS) containing 25% sucrose. After centrifugation, the bacterial cells were incubated in 25 mL of 5 M LiCl to strip the surface-associated proteins. After treatments, the cells were collected and washed three times with autoclave sterilized seawater.

2.2. Feeding trials

The experimental diets were prepared as previously described: bacteria were resuspended in sterilized seawater and sprayed on basal commercial feed (containing crude protein 42%, crude fat 7%, ash 15%, and water 11%) at 5×10^8 colony-forming units (CFU) g/feed [22]. A total of 600 shrimp (3.5 ± 0.06 g) were grown in twelve aquaria (60 L), each containing 50 shrimp. The experiments were designed as follows: Control group, shrimp fed a basal commercial diet; R group, shrimp fed a basal commercial diet + normal HC-2; L group, shrimp fed a basal commercial diet + LiCl-treated HC-2. Three replicates were used in each feeding group. The seawater was kept fresh (salinity, 30‰) at 30 ± 2 °C with continuous aeration and a 50% water change every day. The animals were fed three times per day, and the daily feeding rate was 10% of the body weight. Four weeks of breeding were conducted after the shrimp had been acclimated for one week.

2.3. Challenge test

After the feeding experiment, 25 shrimp were randomly selected from each aquarium and transferred to a tank with 30 L of seawater for the challenge test. The live *Vibrio parahaemolyticus* E1 ATCC 17,802 strain was used for the challenge and cultured aerobically in 2216 E broth (Qingdao Hope Biol-Technology Co., Ltd) at 28 °C for 18 h. A preliminary experiment showed that the appropriate bacterial dose was 10^7 CFU/mL. The challenge test was carried out continuously for 3 days, the water was changed once a day, and the concentration of bacteria was reformulated. The shrimp were fed a basic diet during the challenge experiment.

2.4. Histology of the midgut

The histology was performed as described by Sha et al. (2016) [20]. Five shrimp were freely selected from each treatment group upon termination of the feeding and challenge experiments, and the midguts were sampled for dissection and fixation (60% absolute ethanol, 30% trichloromethane, 10% acetic acid) for 19 h. Then, the fixed tissues were dehydrated in ascending concentrations of alcohol (70, 80, 95, and 100%), cleared in toluene, embedded in paraffin, and sectioned at 10 μm with a rotary microtome. The sectioned tissues were stained with hematoxylin and eosin, and images were obtained with a light microscope.

2.5. Protein extraction and separation by 1D gel electrophoresis

Upon termination of the feeding experiment, the midguts of twenty shrimp from each treatment group were dissected, and the intestinal contents were removed by flushing with sterile precooled PBS. Total intestine proteins were extracted as described by Sengupta et al. (2011) [23] with some modifications. Pooled samples (1 g) were thoroughly ground into fine powder in liquid nitrogen with a mortar and pestle and dissolved in 5 mL extraction buffer (0.5 M Tris-HCl (pH 7.5), 0.7 M sucrose, 0.1 M KCl, 50 mM EDTA, 40 mM DTT) at room temperature for 15 min. After adding an equal volume of Tris-phenol and shaking for 30 min, the upper phenolic phase was collected by centrifugation (8000 × *g*) for 5 min at 4 °C, and an equal volume of extraction buffer was added to the supernatant. Four volumes of 0.1 M ammonium acetate in methanol were added and incubated at −20 °C overnight to precipitate the proteins. The protein pellet was collected after centrifugation at 8000 × *g* for 10 min at 4 °C and washed three times with ice-cold acetone at 4 °C. The pellet was dried under vacuum for 2 h and then solubilized in 100 μL rehydration solution (8 M (w/v) urea, 0.1 M (w/v) Tris, 10 mM DTT). The concentration of protein was determined using the Bradford method [24]. Finally, proteins were loaded on 10% SDS-PAGE, separated at 120 V for 2 h, and visualized using colloidal Coomassie blue after electrophoresis.

2.6. Trypsin in-gel digestion

Protein gels were washed three times with 50% acetonitrile (ACN)/50% NH_4HCO_3 (100 mM) for 10 min to destain and dried in a vacuum concentrator. The gels were dissolved in 200 μL 10 mM DTT containing 50 mM NH_4HCO_3 (pH 8.0) for 1 h at 37 °C and then destained by 100 μL acetonitrile (ACN). Then, alkylation was performed with 55 mM iodoacetamide (Sigma-Aldrich)/50 mM NH_4HCO_3 (pH 8.0) for 30 min in the dark. The gel bands were alternately washed twice with 10 mM NH_4HCO_3 and 100% ACN. The gels were dried by a Speed-Vac and digested with trypsin (0.01 μg/μl) (Promega, Madison, WI) in 10 mM NH_4HCO_3 at 37 °C overnight. Digestion was stopped by adding 60% ACN/5% formic acid (FA).

Table 1
Primers used in the validation experiment.

Gene ID	Gene name	Primer sequence (5′-3′)	Product size (bp)
	β-Actin	F-GCCCATCTACGAGGGATA R-GGTGGTCGTGAAGGTGTAA	121
Cluster-14773.30,853_orf1	Hemocyanin	F- CCCAAGGGCAACGATAGAGGC R- GGAACTTTGCGGTCCAGAGGA	173
Cluster-14773.45,179_orf1	C1q-binding protein	F- TATGAGTGCCATCAGTCGTGC R- CAAGTTCCTCGTCAGGTTTCG	109
Cluster-14773.30,841_orf1	Calreticulin	F- ATACCTCATTATGTTTGGTCCTG R- TCGTCCTTACAACGGATTTCT	117
Cluster-14773.30,587_orf1	Pyruvate kinase 2	F- CCCCACTGGTCGCTCTGCTCAT R- CAACAGGGTCGCCGGGCTTAA	245
Cluster-14773.29,642_orf1	Integrin	F- TAGTGGTAGCAGTTCCGAAGA R- GAGATAATAAAGGTCAACAGGGT	139
Cluster-14773.32,147_orf1	Proliferating cell nuclear antigen	F- CAAAGAGGAGGAAGCAGTCGT R- CATAGAAAGTGAAACCTGTGGG	121
Cluster-14773.34,990_orf1	Hemocyte transglutaminase	F- CCCGCTAAATGGCTCGGTTCT R- TTGGTCACGACACGGCAAGGT	146

2.7. Nanoflow liquid chromatography-tandem mass spectrometry

Prior to analyzing the tryptic digest extracts using a Thermo Scientific EASY-nLC 1000 System (Nano HPLC), the crude polypeptides were first desalted with a ChromXP trap column (Nano LC TRAP Column, 3 μm C_{18}-CL, 120 A, 350 μm × 0.5 mm, Foster City, CA, USA) and then eluted onto a second analytical column of a Nano LC C_{18} reversed-phase column (3C 18-CL, 75 μm × 15 cm, Foster City, CA, USA) under a linear gradient formed by mobile phases A (5% ACN and 0.1% FA) and B (95% CAN and 0.1% FA) at a flow rate of 300 nL/min for 120 min. Triple TOF 5600 MS (Foster City, CA, USA) was performed automatically switch the TOF-MS and production acquisition in data in TFR-dependent mode by Analyst (R) Software (TF1.6).

2.8. Protein identification

Three biological replicates were performed for the control, R and L groups. The LC-MS/MS raw data were processed using MaxQuant (version 1.5.2.8) for peptide/protein identification and quantification. MS/MS spectra were searched by the Andromeda search engine using a database consisting of 28,384 sequences of the shrimp transcriptome downloaded from NCBI. The search parameters were as follows: monoisotopic mass values; enzyme was trypsin; static modification with C carboxyamidomethylation (57.021 Da); dynamic modification was M Oxidation (15.995 Da); precursor ion mass tolerance ± 15 ppm; fragment ion mass tolerance with ± 20 mmu; allowance of two missed cleavage sites; false discovery rate (FDR) set as 0.01. Peptides identified with 95% confidence are considered “significant sequences”. For protein quantification, a minimum of two ratio counts was set to compare and normalize protein intensities across runs [25]. The absolute abundance of different proteins was then calculated using the intensity-based absolute quantification (iBAQ) algorithm, and iBAQ data were used for the *t*-test [26].

2.9. Bioinformatics analysis

Gene ontology (GO) enrichment and Kyoto Encyclopedia of Genes and Genomes (KEGG) annotation for each protein in the search database were analyzed in GO (http://www.geneontology.org/) and the KEGG Pathway database (http://www.genome.jp/Pathway), respectively. The GO project provides three types of ontology analyses, namely, molecular functions (MF), cellular components (CC), and biological process (BP) [27]. Subcellular localization for each protein was predicted according to GO annotation by UniProt software (http://www.uniprot.org/). GO items without corresponding annotation were first deleted from the protein table, and then the IDs of listed proteins were plotted at the BP, CC, and MF levels. In addition, differentially expressed proteins (fold changes > 1.5, $p < 0.05$) were mapped to the GO database, and the number of proteins at each GO term was computed. The results from label-free proteomics were used as the target list. The background list was generated by downloading the GO database.

2.10. Quantitative real-time PCR

RNA was prepared from the midguts of ten *L. vannamei* that had been used for real-time PCR analysis. Total RNA was extracted using an E. Z.N.A. HP Total RNA Kit (Omega Bio-Tek, Norcross, GA, USA) and subjected to reverse transcription to create first-strand cDNA using the RevertAid First Strand cDNA Synthesis Kit (Thermo Fisher Scientific) according to the manufacturer's instructions. Seven proteins, including hemocyanin (Hem), C1q-binding protein (C1q), calreticulin (Cal), pyruvate kinase 2 (Pyr), integrin (Int), proliferating cell nuclear antigen (Pro), and hemocyte transglutaminase (Htr), were selected for the determination of their mRNA levels, all of which were annotated to *L. vannamei* and were important proteins functioning in the immune response, metabolism, adhesion and cell-cell signaling. The primer sequences were designed by Primer 5 (Table 1). The reactions were carried out using Bio-Rad IQ™5 real-time PCR with a total volume of 20 m L (2*SYBR Green Mix (Vazyme Biotech): 10 m L, primer: 1.0 m L, cDNA template: 5.0 m L, and PCR-grade water: 4.0 m L). The qRT-PCR procedure was as follows: initial denaturation at 95 °C for 2 min; 40 cycles of amplification (95 °C for 15 s, 60 °C for 20 s, and 72 °C for 20 s). The cycle threshold (Ct) was measured, and the relative gene expression was calculated using the $2^{-\triangle\triangle Ct}$ method. The *β*-actin gene was used as an endogenous control. Three biological replicates and three technical replicates were performed for all PCR experiments, and significance was determined at $P < 0.05$.

3. Results

3.1. Histology of the midgut

To investigate the effects of dietary LiCl-treated probiotics on the midgut of the shrimp, a histological study was performed at the end of the feeding experiment and challenge assay as shown in Fig. 1. Compared with the control group, the mucosae of the R group improved more densely and had more blooms (Fig. 1B), but the mucosae of the L group shrimps displayed as thin and loose (Fig. 1C). After the shrimp were challenged by *V. parahaemolyticus* E1, the mucosae shed and piled in the intestinal lumen; the lamina propria exposed and appeared loose in the control and L groups (Fig. 1D and F), and some individuals

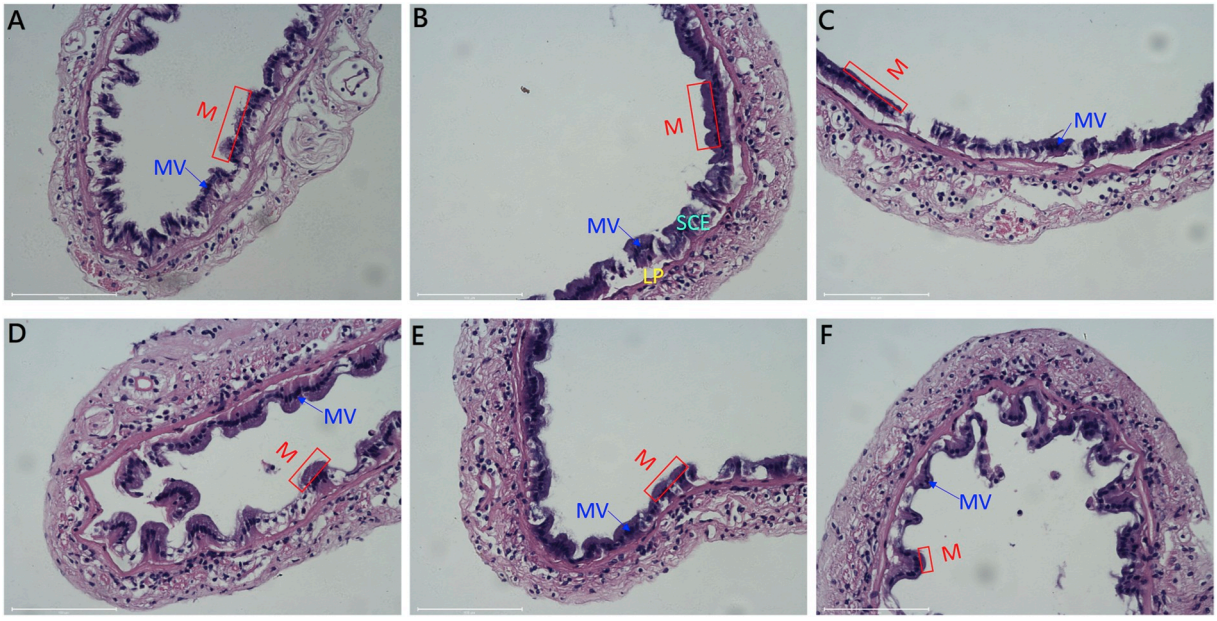

Fig. 1. Histology with hematoxylin and eosin staining of the shrimp midguts after feeding with different diets for 4 weeks. Images A, B, C, D, E and F are arbitrarily chosen examples of the histology observed in three groups. A: Gut histology of shrimp fed a basic diet; B: Gut histology of shrimp fed a basic diet supplied with normal *L. pentosus* HC-2; C: Gut histology of shrimp fed a basic diet supplied with LiCl-treated *L. pentosus* HC-2; D, E and F showed the gut histology of shrimp in A, B and C, respectively, which were challenged by *Vibrio parahaemolyticus* E1. LP: lamina propria, M: mucosae, MV: microvilli, SCE: surface cell epithelium. Bar: 100 μm.

showed reduced folding of the digestive epithelium in the crease. However, the shrimp fed normal HC-2 appeared to have no signs of necrotic enterocytes or cell damage (Fig. 1E).

3.2. Label-free proteomic analysis of the intestinal proteins of L. vannamei

In total, 2810 proteins were detected. The differential protein expression among the three groups is shown in the S1 Appendix, and proteins with fold changes $\geq \pm 1.5$ and $P < 0.05$ were considered significantly differentially abundant. Pairwise comparisons of intestinal proteins with different levels among the R/control, L/control, and L/R are illustrated in Fig. 2 and identified 210, 510 and 458 differentially abundant proteins, respectively. The numbers of upregulated proteins were 110, 134, and 85, respectively, whereas 101, 376, and 373 proteins, respectively, were downregulated. The relationships among the experimental groups were determined by a PCoA analysis in the protein expression pattern form. Samples of the control, R and L groups clustered independently (Fig. 3). To comprehensively analyze the impact of HC-2 and LiCl-treated HC-2 on protein expression changes, differentially abundant proteins were subjected to cluster analysis under different experimental conditions (Fig. 4). A heat map showed that samples of the control, R and L groups were clustered. The results of the heat map and PCoA were somewhat consistent, indicating that the protein expression in the control, R and L groups differed and that the protein expression in the midgut was influenced by the addition of HC-2 and LiCl-treated HC-2.

3.3. GO analysis of DEPs in L. vannamei midguts

Based on the gene ontology (GO) analysis in level 2 of biological process, cellular components and molecular functions associated with the significantly differentially abundant intestinal proteins (q-value $<$ 0.05, and log2 |fold change| $>$ 1.5) (Fig. 5). Among the 210 differentially abundant proteins in the R/control comparison; 93 proteins played a role in 23 different biological processes; 139 proteins were related to cellular components, and 46 proteins had distinct molecular functions. Compared with the control group, 510 differentially abundant proteins in the L group comprised 189 proteins that participated in

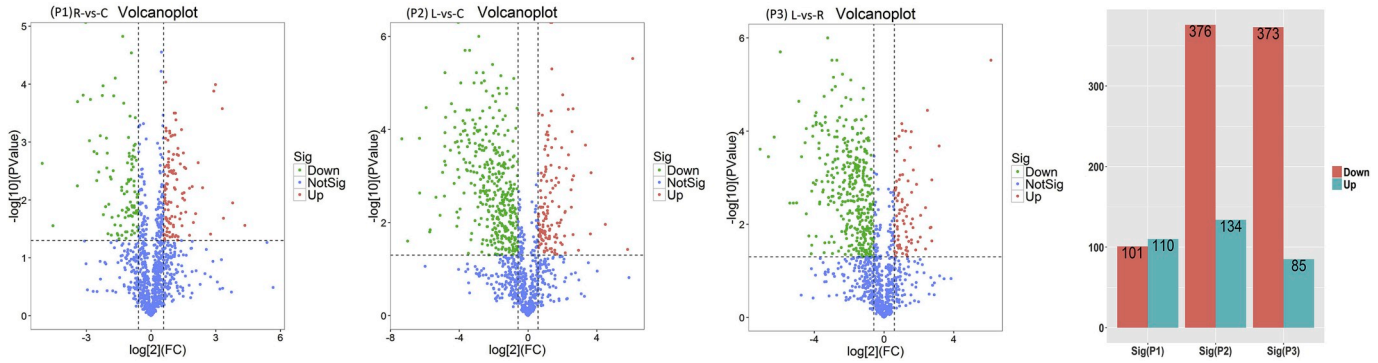

Fig. 2. Volcano plot of changes in the levels of identified intestine proteins of shrimp analyzed using label-free quantitative proteomics after feeding with different diets. Note: C, shrimp were fed a basal diet; R, shrimp were fed a basal diet supplemented with normal *L. pentosus* HC-2; L, shrimp were fed a basal diet supplemented with LiCl-treated *L. pentosus* HC-2.

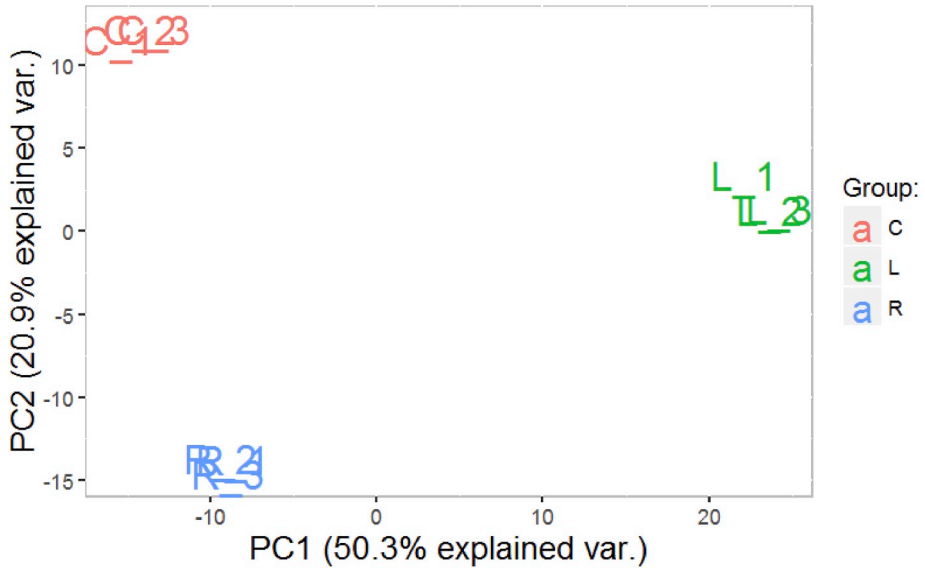

Fig. 3. Principal coordinates analysis scores based on the UniFrac distance. PC1: the first principle component; PC2: the second principle component. Shrimp were fed a basal diet (C) or a basal diet supplemented with *L. pentosus* HC-2 (R), LiCl-treated *L. pentosus* HC-2 (L).

25 biological processes; 100 proteins had specific molecular functions, and 318 proteins were related to cellular components. Biological process analysis indicated that the transport, signal transduction, reproduction, immune system process, protein transport, transmembrane transport, embryo development, cell cycle, cell death, carbohydrate metabolic process, vesicle-mediated transport, growth, protein targeting, cell-cell signaling and cell-adhesion processes involved the majority of proteins in the R/control or L/control comparisons. Cellular component analysis of the R/control and L/control comparisons revealed that the main differentially abundant proteins belonged to the cytoplasm, membrane, nucleus, plasma membrane, mitochondrion, cytoskeleton, extracellular region and endoplasmic reticulum.

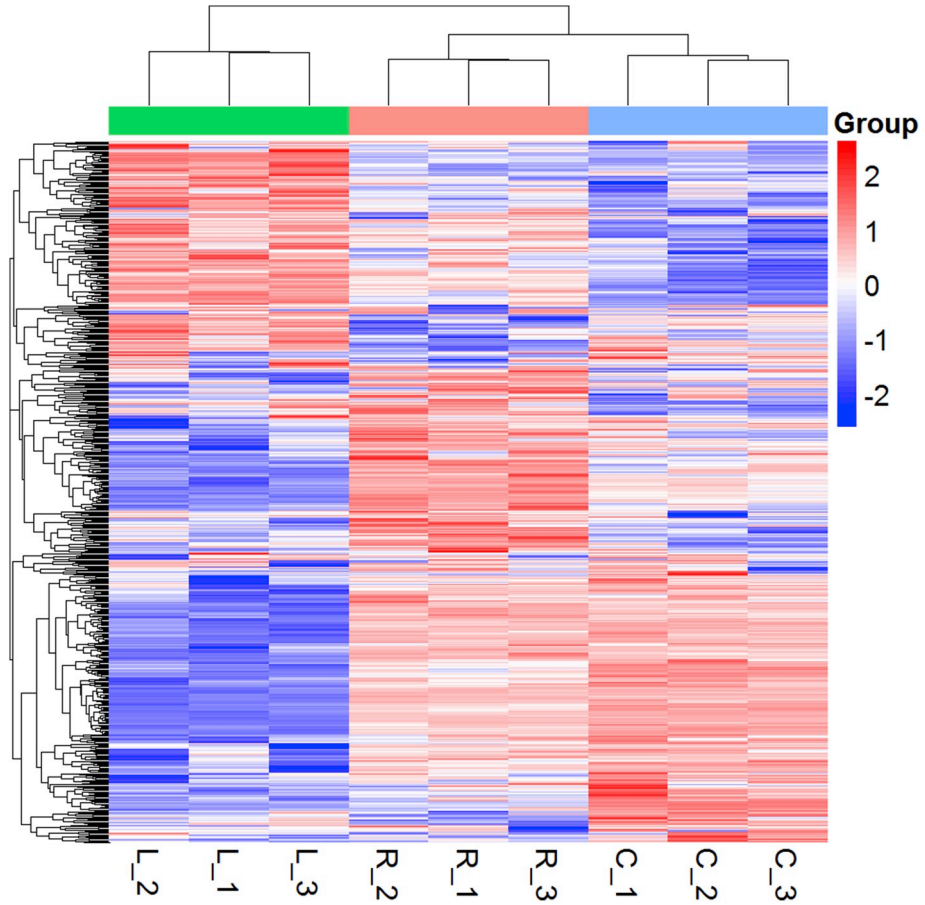

Fig. 4. Heat map of the protein expression diversity among the three groups (9 samples). Shrimp were fed a basal diet (C [C1, C2, C3]) or a basal diet supplemented with normal *L. pentosus* HC-2 (R [R1, R2, R3]) and LiCl-treated *L. pentosus* HC-2 (L [L1, L2, L3]).

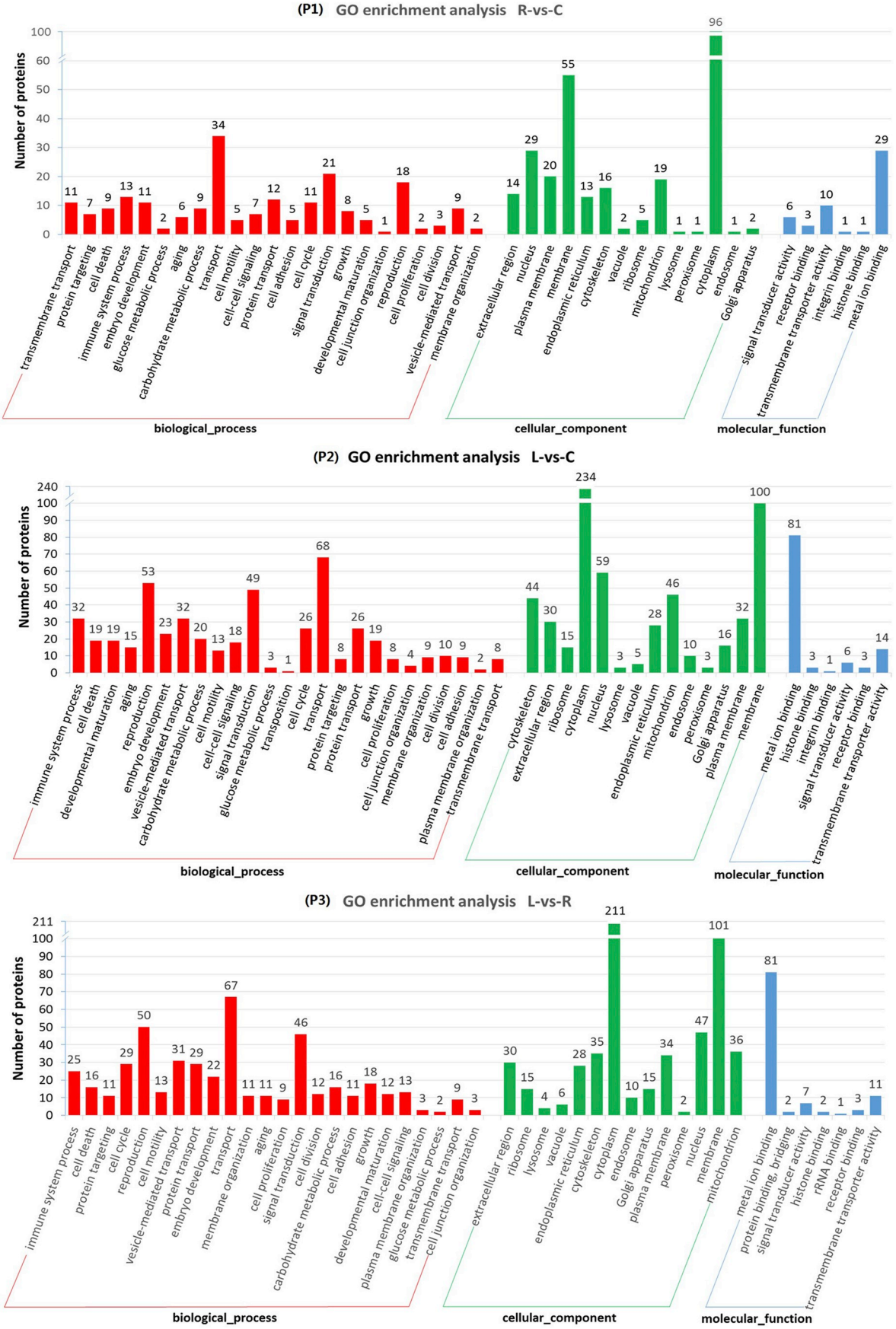

Fig. 5. Functional categorization based on gene ontology (GO) in biological process, cellular components and molecular function level analysis of significantly differentially abundant intestinal proteins. Shrimps were fed a basal diet (C) or a basal diet supplemented with *L. pentosus* HC-2 (R), LiCl-treated *L. pentosus* HC-2 (L).

Molecular function analysis revealed that most differentially abundant proteins were related to metal ion binding and transmembrane transporter activity in both the R/control and L/control comparisons. Comparing L to R, 177 proteins played roles in the biological processes of transport, reproduction, signal transduction, vesicle-mediated transport, cell cycle, protein transport, immune system process, embryo development, growth, cell death, carbohydrate metabolic process, cell motility, cell-cell signaling, cell division, developmental maturation, protein targeting, membrane organization, and cell adhesion. The cellular components of 290 differentially abundant proteins were cytoplasm, membrane, nucleus, mitochondrion, cytoskeleton, plasma membrane, extracellular region, endoplasmic reticulum, ribosome and Golgi apparatus; and 100 differentially abundant proteins in the molecular function categories were related to metal ion binding, transmembrane transporter activity and signal transducer activity.

3.4. KEGG pathway analysis of the DEPs in L. vannamei midguts

KEGG pathway analysis was performed to determine the biological pathways that involved the differentially abundant proteins (q-value < 0.05, and log2 |fold change| > 1.5) induced by HC-2 and LiCl-treated HC-2 treatments fed the diet (Fig. 6). The DEPs between the R group and the control group were mainly enriched in the mTOR signaling pathway, ECM-receptor interaction, RNA degradation, apoptosis, phagosome, butanoate metabolism and oxidative phosphorylation. The DEPs between the L and control groups were mainly enriched in protein processing in the endoplasmic reticulum, RNA transport, tyrosine metabolism, arginine and proline metabolism, lysosome, mRNA surveillance pathway, cysteine and methionine metabolism and glutathione metabolism. The DEPs between the R and L groups were mainly enriched in protein processing in the endoplasmic reticulum, endocytosis, ribosome, lysosome, glycolysis/gluconeogenesis, cysteine and methionine metabolism and tyrosine metabolism.

3.5. Proteins potentially involved in shrimp immune response, metabolic, cell-adhesion and cell-signaling processes

The GO enrichment analysis of the biological processes of the significantly different proteins involved in shrimp immune system processes, cell-cell-signaling processes, cell adhesion and carbohydrate metabolic processes among the three groups is shown in Table 2. In the R/control group, 10 proteins involved in immune system processes, 7 proteins involved in cell-cell-signaling processes, 5 proteins involved in cell adhesion and 4 proteins involved in carbohydrate metabolic processes were significantly increased, and 5 proteins involved in immune and carbohydrate metabolic processes were significantly decreased. Among them, tyrosine-tRNA ligase, C1q-binding protein, tyrosine-protein phosphatase 69 D-like and neutral alpha-glucosidase AB were upregulated the most in the four processes in which the expression levels reached 10.28-, 5.66-, 2.88- and 6.77-fold, respectively. However, in the L/control group, there was no increase in protein upregulation, and 22, 12, 6 and 18 proteins participated in immune, cell-cell signaling, cell adhesion and carbohydrate metabolic processes, respectively, and were significantly downregulated.

Based on the KEGG enrichment analysis, several of the proteins that were differentially expressed in shrimp fed probiotics are involved in the immune system process (mTOR signaling pathway, apoptosis, phagosome, oxidative phosphorylation, MAPK signaling pathway, lysosome, protein processing in endoplasmic reticulum), metabolism process (arginine and proline metabolism, tyrosine metabolism, glutathione metabolism, glycerolipid metabolism/histidine metabolism, cysteine and methionine metabolism, fatty acid metabolism, carbon metabolism), cell-adhesion process (focal adhesion, tight junction, ECM-receptor interaction), and cell-signaling process (calcium signaling pathway, oxytocin signaling pathway, FoxO signaling pathway and Wnt signaling pathway) (Table 3).

3.6. Analysis of selected proteins affected by HC-2 and LiCl-treated HC-2 treatments

To validate the label-free-based proteomic results, quantitative real-time PCR was used to analyze the transcripts of proteins found to be differentially abundant after HC-2 and LiCl-treated HC-2 treatments (Fig. 7). The qPCR results showed that three proteins (Int, Pro and Htr) were expressed at higher levels than determined in the R group proteome, and the other proteins were consistent with the proteomics data, which further confirmed the reliability of the label-free sequence.

4. Discussion

The gastrointestinal tract, the most important digestive and absorption organ in shrimps, contains large numbers of microorganisms with complex structures. These organisms depend on and restrict each other with hosts, forming a unique intestinal microecosystem during the long process of evolution [28]. In recent years, it has been widely recognized that supplementation with probiotics in aquaculture may stabilize the indigenous microflora and normalize the host-microbe interaction, which contributes to reducing the incidence of diseases [29]. Our previous work demonstrated that *L. pentosus* HC-2 has an ideal probiotic effect on *L. vannamei*, but the probiotic action of HC-2 surface components to shrimp is not clear. To investigate the impact of surface proteins on the probiotic effect of HC-2 on *L. vannamei*, proteomic analyses were conducted using a label-free based LC-MS/MS approach to obtain protein data from three biological replicates.

Several studies demonstrated that dietary probiotic supplementation could improve the growth performance, which was deemed to be attributed to intestinal physiology and gut epithelial morphology changes [30,31], such as an improved intestinal microvillus structure and a greater absorptive surface area [32,33]. In the present study, the changes in the intestinal microvilli and the folding of the digestive epithelium varied between dietary groups, and obvious improvement in intestinal histology was observed after the shrimp were fed the normal probiotic HC-2, and the intestinal tissue was not damaged after the shrimp were challenged by *V. parahaemolyticus* E1. These results are similar to the findings of Merrifield et al. (2010) [33], who found that *Pediococcus acidilactici*-fed fish had significantly longer microvilli than other groups of fish, but differ from the findings of Sha et al. (2016) [20], who reported that dietary HC-2 did not improve the intestinal morphology of *L. vannamei*. These different phenomena may be attributable to a lower bacterial concentration used in the dietary diet (10^7 CFU/g) than that used in this work (5×10^8 CFU/g), which hinders the ability of HC-2 to be the dominant microflora in the shrimp intestines to improve the intestinal morphology. However, there was no sign of improvement in intestinal histology after the shrimp were fed LiCl-treated HC-2; instead, the mucosae were thin and loose after the shrimp were challenged by pathogens and were in even worse shape than the control shrimp. These results indicated that surface proteins play important roles in the probiotic function of HC-2 to improve gut physiology and morphology.

With the intensive development of aquaculture and frequent outbreaks of disease, varied probiotics have been developed to meet the demand for pollution-free immune enhancers. In shrimp farming, many researchers have studied the influence of probiotics on the immune response. For example, Wang et al. (2010) [34] indicated that shrimp fed *Lactobacillus* had enhanced growth performance, increased digestive enzyme activities, and increased nonspecific immunity. Zheng et al. (2017) [35] also revealed that the administration of *Lactobacillus pentosus* AS13 effectively improved shrimp growth performance, feed utilization, digestive enzymes and disease resistance. In the present work, proteomic analysis showed that feeding with normal HC-2 induced proteins involved in immune system process (mTOR signaling pathway, apoptosis, phagosome, oxidative phosphorylation, MAPK signaling pathway, lysosome, and protein processing in the endoplasmic

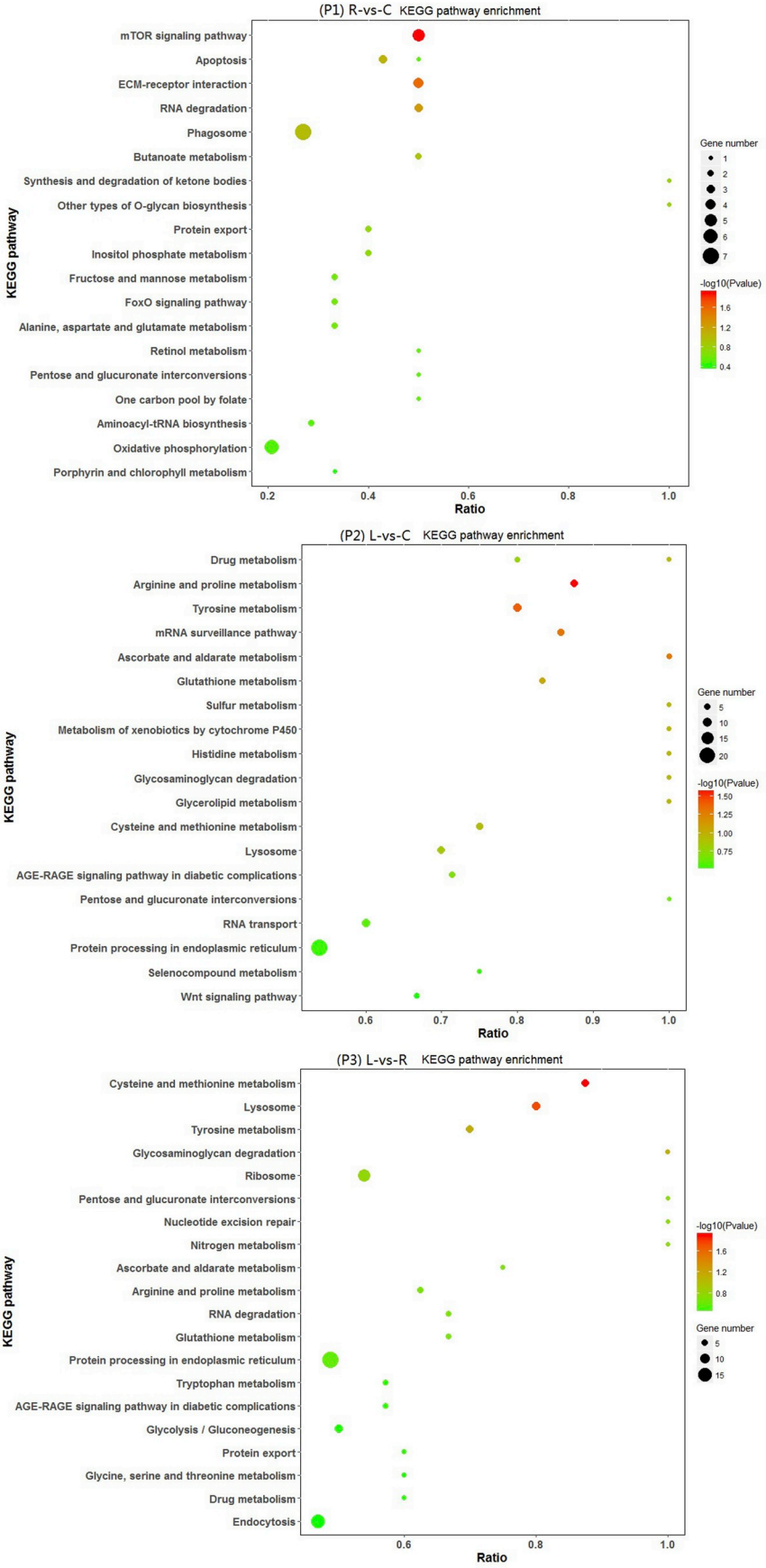

Fig. 6. Distribution of the differentially abundant proteins in the shrimp midgut in KEGG pathways (Top 20). Note: Shrimp were fed a basal diet (C) or a basal diet supplemented with *L. pentosus* HC-2 (R), LiCl-treated *L. pentosus* HC-2 (L).

Table 2
GO enrichment analysis of the significantly difference proteins related immune system process, cell-cell signaling and cell adhesion in among the three experiments group.

ID	Description	Species	R-VS-C		L-VS-C		L-VS-R	
			Ratio	pValue	Ratio	pValue	Ratio	pValue
Immune system process								
Cluster-14773.11824_orf1	Laminin subunit beta-1	*Zootermopsis nevadensis*	2.74	0.01	1.96	0.04	0.72	0.01
Cluster-14773.25451_orf1	polymerase 2	*Larimichthys crocea*	2.16	0.04	3.00	0.03	1.39	0.26
Cluster-14773.29283_orf1	program cell death 5-like	*Penaeus monodon*	1.92	0.00	2.06	0.01	1.07	0.48
Cluster-14773.30313_orf1	alpha-tubulin	*Eriocheir sinensis*	1.67	0.00	1.61	0.00	0.97	0.68
Cluster-14773.34529_orf1	hemocyte protein-glutamine gamma-glutamyltransferase	*Tribolium castaneum*	1.59	0.00	1.93	0.00	1.21	0.09
Cluster-14773.34990_orf1	hemocyte transglutaminase	*Litopenaeus vannamei*	2.30	0.00	3.41	0.00	1.48	0.01
Cluster-14773.31474_orf1	Dolichyl-diphosphooligosaccharide-protein glycosyltransferase subunit 2	*Zootermopsis nevadensis*	1.56	0.01	1.08	0.41	0.69	0.01
Cluster-14773.24787_orf1	tyrosine-tRNA ligase	*Ciona intestinalis*	10.28	0.02	0.69	0.47	0.07	0.02
Cluster-43580.1_orf1	Laminin subunit alpha	*Zootermopsis nevadensis*	1.75	0.02	1.10	0.66	0.63	0.01
Cluster-14773.25609_orf1	DDX6, partial	*Eriocheir sinensis*	1.58	0.00	0.25	0.00	0.16	0.00
Cluster-14773.19715_orf1	hemocytin	*Microplitis demolitor*	1.12	0.24	2.33	0.00	2.08	0.00
Cluster-14773.32036_orf1	Pro-interleukin-16	*Zootermopsis nevadensis*	2.12	0.09	3.79	0.01	1.78	0.02
Cluster-14773.35026_orf1	polymerase	*Athalia rosae*	1.72	0.03	3.19	0.02	1.86	0.03
Cluster-14773.26871_orf1	peroxiredoxin-5	*Palaemon carinicauda*	1.62	0.09	1.87	0.01	1.15	0.33
Cluster-14773.29714_orf1	cytochrome B5	*Ixodes scapularis*	0.64	0.10	0.36	0.00	0.56	0.21
Cluster-14773.31173_orf1	Transportin-1	*Zootermopsis nevadensis*	0.94	0.70	0.35	0.05	0.37	0.05
Cluster-14773.33092_orf1	hemocyanin	*Fenneropenaeus chinensis*	0.40	0.06	0.11	0.00	0.28	0.27
Cluster-14773.32147_orf1	proliferating cell nuclear antigen	*Litopenaeus vannamei*	3.61	0.07	0.28	0.48	0.08	0.00
Cluster-14773.22076_orf1	hemocyanin	*Fenneropenaeus chinensis*	1.14	0.37	0.29	0.00	0.25	0.00
Cluster-14773.26634_orf1	beta-arrestin-1 isoform X3	*Solenopsis invicta*	0.95	0.87	0.16	0.00	0.16	0.04
Cluster-14773.30054_orf1	hemocyanin subunit L1, partial	*Litopenaeus vannamei*	1.65	0.12	0.21	0.05	0.12	0.00
Cluster-14773.30500_orf1	hemocyanin subunit L3, partial	*Litopenaeus vannamei*	0.81	0.02	0.08	0.00	0.10	0.00
Cluster-14773.30709_orf1	hemocyanin subunit L2, partial	*Litopenaeus vannamei*	1.06	0.59	0.11	0.00	0.11	0.00
Cluster-14773.3071_orf1	tubulin alpha-1B chain-like, partial	*Xiphophorus maculatus*	0.70	0.07	0.15	0.00	0.21	0.00
Cluster-14773.30853_orf1	hemocyanin	*Litopenaeus vannamei*	0.95	0.28	0.34	0.00	0.35	0.00
Cluster-14773.30881_orf1	hemocyanin subunit L1, partial	*Litopenaeus vannamei*	0.90	0.02	0.14	0.00	0.15	0.00
Cluster-14773.30960_orf1	hemocyanin subunit L2, partial	*Litopenaeus vannamei*	0.87	0.03	0.13	0.00	0.14	0.00
Cluster-14773.31109_orf1	alpha-III tubulin	*Homarus americanus*	1.30	0.16	0.55	0.00	0.42	0.01
Cluster-14773.32264_orf1	hypothetical protein DAPPUDRAFT_304677	*Daphnia pulex*	0.80	0.23	0.31	0.01	0.39	0.01
Cluster-14773.32691_orf1	Coatomer subunit beta	*Zootermopsis nevadensis*	1.05	0.05	0.55	0.00	0.53	0.00
Cluster-14773.34005_orf1	GTP binding protein alpha subunit Gq	*Marsupenaeus japonicus*	0.95	0.62	0.27	0.00	0.28	0.00
Cluster-14773.41189_orf1	putative serine proteinase inhibitor	*Pacifastacus leniusculus*	0.78	0.03	0.20	0.00	0.25	0.00
Cluster-14773.7946_orf1	hemocyanin subunit L5, partial	*Litopenaeus vannamei*	0.82	0.01	0.40	0.00	0.49	0.00
Cluster-14773.30719_orf1	ribosomal protein S6	*Procambarus clarkii*	0.48	0.01	0.05	0.00	0.09	0.03
Cluster-14773.34255_orf1	AAEL004176-PA	*Aedes aegypti*	0.24	0.00	0.13	0.00	0.52	0.00
Cluster-31172.1_orf1	rho-related GTP-binding protein RhoC	*Danio rerio*	0.66	0.09	1.93	0.04	2.38	0.04
cell-cell signaling								
Cluster-14773.31217_orf1	Ankyrin-2	*Zootermopsis nevadensis*	2.83	0.00	4.65	0.00	1.64	0.09
Cluster-14773.29943_orf1	heterogeneous nuclear ribonucleoprotein R isoform X3	*Solenopsis invicta*	2.33	0.01	3.47	0.01	1.49	0.09
Cluster-14773.34699_orf1	calcium-transporting ATPase	*Cherax cainii*	1.60	0.00	2.06	0.00	1.29	0.01
Cluster-14773.30714_orf1	AAEL000410-PA	*Aedes aegypti*	1.76	0.01	0.99	0.95	0.56	0.07
Cluster-14773.26387_orf1	Exocyst complex component 4	*Zootermopsis nevadensis*	1.43	0.01	1.59	0.01	1.11	0.25
Cluster-14773.30511_orf1	GTP binding protein alpha subunit Go	*Marsupenaeus japonicus*	1.41	0.17	1.61	0.01	1.14	0.39
Cluster-14773.45179_orf1	C1q-binding protein	*Litopenaeus vannamei*	5.66	0.01	6.25	0.00	1.10	0.85
Cluster-14773.21680_orf1	Phospholipid scramblase 2	*Zootermopsis nevadensis*	0.90	0.45	0.60	0.04	0.67	0.02
Cluster-14773.23696_orf1	hypothetical protein DAPPUDRAFT_300160	*Daphnia pulex*	0.73	0.41	0.14	0.00	0.19	0.12
Cluster-14773.29885_orf1	protein kinase C and casein kinase substrate in neurons protein 1	*Tribolium castaneum*	0.82	0.58	0.26	0.01	0.31	0.02
Cluster-14773.19509_orf1	rho-related GTP-binding protein RhoC	*Danio rerio*	1.56	0.02	0.74	0.05	0.48	0.02
Cluster-14773.26929_orf1	AGAP003725-PB-like protein	*Anopheles sinensis*	1.30	0.16	0.76	0.07	0.58	0.03
Cluster-14773.32473_orf1	S-phase kinase-associated protein 1	*Eriocheir sinensis*	2.14	0.01	0.08	0.11	0.04	0.00
Cluster-14773.29557_orf1	microtubule-actin cross-linking factor 1 isoform X17	*Vollenhovia emeryi*	1.14	0.21	0.58	0.02	0.50	0.01
Cluster-14773.30945_orf1	Rab GDP dissociation inhibitor alpha	*Zootermopsis nevadensis*	0.68	0.01	0.37	0.00	0.55	0.04
Cluster-14773.30964_orf1	twinfilin	*Tribolium castaneum*	0.91	0.37	0.24	0.00	0.26	0.01
Cluster-14773.33764_orf1	hypothetical protein BRAFLDRAFT_229359	*Branchiostoma floridae*	0.92	0.48	0.50	0.00	0.54	0.00
Cluster-14773.34005_orf1	adenine nucleotide translocase 2	*Litopenaeus vannamei*	0.95	0.62	0.27	0.00	0.28	0.00
Cluster-14773.34570_orf1	Spectrin alpha chain	*Zootermopsis nevadensis*	0.98	0.84	0.10	0.00	0.10	0.00
Cluster-14773.31084_orf1	Phospholipid scramblase 2	*Zootermopsis nevadensis*	0.31	0.33	0.08	0.00	0.26	0.27
Cluster-14773.32020_orf1	baiser CG11785-PA protein	*Blattella germanica*	0.58	0.11	0.25	0.00	0.43	0.03
Cluster-31172.1_orf1	guanine nucleotide-binding protein subunit alpha, other	*Fonticula alba*	0.66	0.09	1.93	0.04	2.38	0.04
cell adhesion								
Cluster-14773.26854_orf1	GTP binding protein alpha subunit Go	*Marsupenaeus japonicus*	2.74	0.01	1.96	0.04	0.72	0.01
Cluster-14773.36988_orf1	tyrosine-protein phosphatase 69D-like	*Apis mellifera*	2.88	0.01	4.40	0.01	1.53	0.07
Cluster-14773.47749_orf1	Thrombospondin-3 precursor	*Pediculus humanus corporis*	2.14	0.00	3.12	0.00	1.45	0.01
Cluster-14773.28858_orf2	suppressor of profilin 2	*Scylla paramamosain*	1.75	0.02	1.10	0.66	0.63	0.01
Cluster-14773.35130_orf1	Catenin alpha	*Zootermopsis nevadensis*	0.48	0.32	1.18	0.70	2.45	0.05
Cluster-14773.32485_orf1	guanine nucleotide-binding protein subunit gamma-1	*Athalia rosae*	1.46	0.07	1.70	0.03	1.16	0.25
Cluster-14773.30621_orf1	hypothetical protein DAPPUDRAFT_41019, partial	*Daphnia pulex*	1.43	0.03	0.87	0.19	0.61	0.01
Cluster-14773.37548_orf1	matrix metalloproteinase 1 isoform 1	*Bombyx mori*	1.16	0.70	0.30	0.14	0.26	0.00
Cluster-30499.0_orf1	guanine nucleotide-binding protein subunit alpha	*Fonticula alba*	1.75	0.02	0.65	0.19	0.37	0.01
Cluster-14773.28018_orf1	hypothetical protein DAPPUDRAFT_308937	*Daphnia pulex*	0.80	0.23	0.31	0.01	0.39	0.01
Cluster-14773.31009_orf1	neuroplastin isoform X1	*Acyrthosiphon pisum*	1.05	0.82	0.20	0.01	0.19	0.00
Cluster-14773.31788_orf1	hypothetical protein DAPPUDRAFT_305821	*Daphnia pulex*	0.71	0.33	0.02	0.01	0.03	0.00

(*continued on next page*)

Table 2 (*continued*)

Cluster-14773.32339_orf1	presenilin-1 isoform X2	*Microplitis demolitor*	**0.81**	0.02	0.47	0.00	0.58	0.01
Cluster-14773.34695_orf1	Nidogen-2	Zootermopsis nevadensis	**1.32**	0.01	0.60	0.01	0.45	0.00
Cluster-14773.32900_orf1	conserved hypothetical protein	*Pediculus humanus corporis*	**0.39**	0.24	0.68	0.19	1.75	0.00
carbohydrate metabolic process								
Cluster-14773.28921_orf1	phosphopyruvate hydratase	*Penaeus monodon*	1.69	0.01	0.60	0.01	0.36	0.00
Cluster-14773.30206_orf1	Glycogen debranching enzyme	*Zootermopsis nevadensis*	1.60	0.01	0.33	0.01	0.21	0.00
Cluster-14773.35902_orf1	alpha-N-acetylgalactosaminidase isoform X2	*Harpegnathos saltator*	**1.34**	0.06	2.03	0.00	1.51	0.01
Cluster-14773.29903_orf1	Neutral alpha-glucosidase AB	*Zootermopsis nevadensis*	6.77	0.01	10.08	0.00	**1.49**	0.45
Cluster-14773.21418_orf1	Phosphoacetylglucosamine mutase	*Zootermopsis nevadensis*	**0.82**	0.22	0.53	0.05	**0.65**	0.11
Cluster-14773.30513_orf1	Phosphoglycerate mutase 2	*Zootermopsis nevadensis*	**0.89**	0.61	**0.59**	0.12	0.66	0.05
Cluster-14773.30660_orf1	putative phosphoglycerate kinase	*Danaus plexippus*	1.83	0.02	**0.58**	0.54	0.32	0.00
Cluster-14773.31213_orf1	hypothetical protein ZHAS_00018295	*Anopheles sinensis*	**1.06**	0.37	**0.67**	0.02	0.63	0.00
Cluster-14773.39230_orf1	hypothetical protein DAPPUDRAFT_306567	*Daphnia pulex*	**1.45**	0.07	**0.44**	0.07	0.31	0.00
Cluster-28467.0_orf1	probable phosphoglycerate kinase	*Hydra vulgaris*	**0.79**	0.76	**0.27**	0.32	0.34	0.04
Cluster-14773.25358_orf1	hypothetical protein DAPPUDRAFT_302911	*Daphnia pulex*	**1.20**	0.67	0.16	0.04	0.13	0.04
Cluster-14773.27702_orf1	glucosamine-6-phosphate isomerase	*Ceratitis capitata*	**0.91**	0.41	0.27	0.00	0.30	0.00
Cluster-14773.27960_orf1	chitinase 1C	*Macrobrachium nipponense*	**1.39**	0.01	0.29	0.00	0.21	0.00
Cluster-14773.28965_orf1	lactate dehydrogenase	*Litopenaeus vannamei*	**0.89**	0.21	0.09	0.00	0.10	0.00
Cluster-14773.30608_orf1	glyceraldehyde-3-phosphate-dehydrogenase	*Cherax cainii*	**1.01**	0.90	0.59	0.04	0.58	0.02
Cluster-14773.31873_orf1	Pyruvate dehydrogenase E1 component subunit beta, mitochondrial	*Zootermopsis nevadensis*	**1.07**	0.72	0.27	0.02	0.26	0.00
Cluster-14773.32166_orf1	6-phosphogluconate dehydrogenase, decarboxylating isoform X1	*Strongylocentrotus purpuratus*	**0.68**	0.07	0.32	0.01	0.46	0.00
Cluster-14773.33708_orf1	hypothetical protein DAPPUDRAFT_303198	*Daphnia pulex*	**1.48**	0.09	0.08	0.00	0.06	0.00
Cluster-14773.27082_orf1	hypothetical protein DAPPUDRAFT_213935	*Daphnia pulex*	**0.58**	0.30	0.53	0.04	**0.92**	0.77
Cluster-14773.30286_orf1	GL19134	*Drosophila persimilis*	**0.16**	0.53	0.21	0.00	**1.30**	0.53
Cluster-14773.30757_orf1	fructose 1,6-biphosphate-aldolase A	*Fenneropenaeus chinensis*	0.24	0.00	0.07	0.00	**0.28**	0.22
Cluster-14773.31441_orf1	fructose 1,6-biphosphate-aldolase A	*Fenneropenaeus chinensis*	0.32	0.00	0.31	0.00	**1.00**	0.97
Cluster-14773.33303_orf1	triose-phosphate isomerase	*Litopenaeus vannamei*	0.03	0.00	0.22	0.02	**7.32**	0.33
Cluster-24630.0_orf1	triosephosphate isomerase, partial	*Obelia sp. KJP-2004*	0.35	0.02	0.22	0.00	**0.63**	0.51
Cluster-32388.0_orf1	beta-N-acetylglucosaminidase	*Fenneropenaeus chinensis*	0.28	0.04	0.18	0.00	**0.63**	0.69

Red shade represent protein was significantly up-regulation, green shade represent protein was significantly down-regulation.

reticulum) upregulation, but many immune-related proteins were downregulated in the LiCl-treated HC-2 group shrimp midgut, suggesting that surface proteins play vital roles in mediating HC-2 to enhance the shrimp intestinal immune response.

Several available genomic information sources described the metabolic activities of lactobacilli, which indicated that surface proteins are important for carbohydrate metabolism in the host [36]. It has been reported that *Lactobacillus paracasei* or *Lactobacillus rhamnosus* probiotic supplementation of HBF in mice exerted microbiome modification and resulted in altered hepatic lipid metabolism coupled with lowered plasma lipoprotein levels and apparent stimulated glycolysis, as well as affecting a diverse range of metabolic pathways, including amino acid

Table 3
KEGG enrichment analysis of the significantly difference proteins related immune system process, metabolism process, adhesion process and signaling process in among the three experiments group.

ID	Description	Species	R-VS-C		L-VS-C		L-VS-R	
			Ratio	pValue	Ratio	pValue	Ratio	pValue
Immune system process								
mTOR signaling pathway								
Cluster-14773.10205_orf1	hypothetical protein BRAFLDRAFT_89962	*Branchiostoma floridae*	1.66	0.04	**0.65**	0.16	0.39	0.01
Cluster-14773.26359_orf1	ras-related GTP-binding protein C	*Nasonia vitripennis*	2.91	0.02	0.54	0.16	0.18	0.04
Cluster-14773.29732_orf1	V-ATPase A	*Cherax destructor*	5.75	0.00	0.23	0.01	**0.04**	0.64
Cluster-14773.30536_orf1	vacuolar ATP synthase subunit g	*Riptortus pedestris*	7.26	0.40	**0.49**	0.10	**0.07**	0.22
Cluster-14773.30719_orf1	ribosomal protein S6	*Procambarus clarkii*	0.48	0.01	0.05	0.00	0.09	0.03
Cluster-31172.1_orf1	rho-related GTP-binding protein RhoC	*Danio rerio*	**0.66**	0.09	0.19	0.00	0.29	0.00
Apoptosis								
Cluster-14773.25451_orf1	poly polymerase 2	*Larimichthys crocea*	2.16	0.04	3.00	0.03	1.39	0.26
Cluster-14773.31501_orf1	caspase 3	*Litopenaeus vannamei*	1.99	0.00	1.86	0.00	0.93	0.45
Cluster-14773.35026_orf1	poly polymerase	*Athalia rosae*	1.72	0.03	3.19	0.02	1.86	0.03
Cluster-14773.28296_orf1	lamin Dm0-like	*Monomorium pharaonis*	**0.49**	0.31	0.18	0.00	0.37	0.00
Phagosome								
Cluster-14773.29660_orf1	protein transport protein Sec61 subunit beta	*Athalia rosae*	**1.16**	0.12	2.92	0.04	2.53	0.05
Cluster-14773.28305_orf1	protein transport protein Sec61 subunit alpha isoform 2	*Aplysia californica*	1.76	0.00	2.53	0.00	**1.44**	0.00
Cluster-14773.30313_orf1	alpha-tubulin	*Eriocheir sinensis*	1.67	0.00	1.61	0.00	**0.97**	0.68
Cluster-41437.0_orf1	actin-1, putative	*Acanthamoeba castellanii str. Neff*	**1.47**	0.11	1.99	0.02	**1.35**	0.18
Cluster-14773.30536_orf1	vacuolar ATP synthase subunit g	*Riptortus pedestris*	7.26	0.40	**0.49**	0.10	**0.07**	0.22
Cluster-14773.29732_orf1	V-ATPase A	*Cherax destructor*	5.75	0.00	0.23	0.01	**0.04**	0.64
Cluster-14773.29890_orf1	beta-II tubulin	*Homarus americanus*	0.30	0.05	0.26	0.03	**0.73**	0.47
Cluster-14773.31428_orf1	cathepsin L	*Penaeus monodon*	1.68	0.03	**1.10**	0.68	0.65	0.01
Cluster-14773.41998_orf1	beta actin	*Aurelia aurita*	2.11	0.00	**1.08**	0.74	0.51	0.01
Cluster-14773.30747_orf1	actin	*Penaeus monodon*	1.88	0.01	**0.69**	0.04	0.37	0.04
Cluster-14773.15936_orf1	beta-II tubulin	*Homarus americanus*	**0.84**	0.50	0.06	0.01	0.08	0.00
Cluster-14773.3071_orf1	tubulin alpha-1B chain-like	*Xiphophorus maculatus*	**0.70**	0.07	0.15	0.00	0.21	0.00
Cluster-14773.30751_orf1	beta-I tubulin	*Homarus americanus*	**0.70**	0.05	0.09	0.00	0.14	0.00
Cluster-14773.31109_orf1	alpha-III tubulin	*Homarus americanus*	**1.30**	0.16	0.55	0.00	0.42	0.01
Cluster-14773.32086_orf1	tubulin, beta, 2	*Danio rerio*	**0.66**	0.06	0.06	0.00	0.09	0.00
Cluster-14773.32462_orf1	Cytoplasmic dynein 1 light intermediate chain 2	*Zootermopsis nevadensis*	**1.40**	0.01	0.42	0.00	0.30	0.00
Cluster-18309.0_orf1	ras-related C3 botulinum toxin substrate 1	*Dipodomys ordii*	**0.81**	0.09	0.44	0.00	0.55	0.00
Oxidative phosphorylation								
Cluster-14773.28421_orf1	ATP-synthase subunit beta	*Schistocerca gregaria*	**0.77**	0.77	2.94	0.04	3.83	0.02
Cluster-14773.34997_orf1	AGAP007297-PA	*Anopheles gambiae str. PEST*	1.95	0.03	3.25	0.01	1.67	0.00
Cluster-14773.28938_orf1	cytochrome c1, heme protein, mitochondrial-like	*Clupea harengus*	1.81	0.00	1.95	0.00	**1.08**	0.09
Cluster-14773.30536_orf1	vacuolar ATP synthase subunit g	*Riptortus pedestris*	7.26	0.40	**0.49**	0.10	**0.07**	0.22
Cluster-14773.30366_orf1	ATP synthase-coupling factor 6, mitochondrial	*Zootermopsis nevadensis*	0.09	0.00	**0.56**	0.35	**5.99**	0.32
Cluster-14773.29732_orf1	V-ATPase A	*Cherax destructor*	5.75	0.00	0.23	0.01	**0.04**	0.64
Cluster-14773.30003_orf1	NADH-ubiquinone oxidoreductase 39 kda subunit	*Culex quinquefasciatus*	2.16	0.02	**0.98**	0.85	0.45	0.02
Cluster-14773.27894_orf1	hypothetical protein DAPPUDRAFT_192333	*Daphnia pulex*	**1.22**	0.06	**0.53**	0.09	0.43	0.03
Cluster-14773.33998_orf1	NADH dehydrogenase iron-sulfur protein 7, mitochondrial	*Zootermopsis nevadensis*	**1.22**	0.50	**0.51**	0.26	0.42	0.05

(*continued on next page*)

Table 3 (*continued*)

Cluster-14773.28639_orf1	NADH-ubiquinone oxidoreductase flavoprotein 1 (ndufv1)	*Anopheles darlingi*	1.60	0.02	0.30	0.01	0.19	0.01
Cluster-14773.29635_orf1	mitochondrial cytochrome c oxidase subunit IV	*Litopenaeus vannamei*	1.12	0.45	0.08	0.00	0.07	0.00
Cluster-14773.29645_orf1	cytochrome b-c1 complex subunit 9	*Tribolium castaneum*	1.10	0.06	0.45	0.00	0.41	0.00
Cluster-14773.30806_orf1	NADH dehydrogenase iron-sulfur protein 3, mitochondrial	*Tribolium castaneum*	0.67	0.00	0.30	0.00	0.45	0.00
MAPK signaling pathway								
Cluster-18309.0_orf1	ras-related C3 botulinum toxin substrate 1	*Dipodomys ordii*	0.81	0.09	0.44	0.00	0.55	0.00
Cluster-14773.21159_orf1	Exportin-1	*Zootermopsis nevadensis*	0.73	0.68	0.16	0.02	0.22	0.37
Cluster-14773.28046_orf1	mitochondrial MnSOD	*Litopenaeus vannamei*	0.86	0.09	0.16	0.00	0.19	0.00
Cluster-14773.30205_orf1	cytosolic MnSOD	*Litopenaeus vannamei*	0.57	0.00	0.31	0.00	0.55	0.00
Cluster-14773.39278_orf1	14-3-3-like protein	*Penaeus monodon*	1.16	0.08	0.71	0.02	0.62	0.00
Lysosome								
Cluster-14773.35902_orf1	alpha-N-acetylgalactosaminidase isoform X2	*Harpegnathos saltator*	1.34	0.06	2.03	0.00	1.51	0.01
Cluster-14773.31428_orf1	cathepsin L	*Penaeus monodon*	1.68	0.03	1.10	0.68	0.65	0.01
Cluster-14773.32773_orf1	N-acetylgalactosamine-6-sulfatase isoform X1	*Takifugu rubripes*	1.56	0.01	0.50	0.00	0.32	0.00
Cluster-14773.28369_orf1	Alpha-N-acetylglucosaminidase	*Zootermopsis nevadensis*	1.07	0.54	0.21	0.00	0.20	0.00
Cluster-14773.30002_orf1	cathepsin D	*Penaeus monodon*	0.87	0.38	0.16	0.00	0.18	0.00
Cluster-14773.31520_orf1	clathrin heavy chain	*Penaeus monodon*	0.97	0.30	0.32	0.00	0.33	0.00
Cluster-14773.33708_orf1	hypothetical protein DAPPUDRAFT_303198	*Daphnia pulex*	1.48	0.09	0.08	0.00	0.06	0.00
Cluster-14773.41103_orf1	AP-3 complex subunit beta-2	*Zootermopsis nevadensis*	1.26	0.16	0.36	0.00	0.28	0.01
Protein processing in endoplasmic reticulum								
Cluster-14773.29660_orf1	protein transport protein Sec61 subunit beta	*Athalia rosae*	1.16	0.12	2.92	0.04	2.53	0.05
Cluster-14773.18758_orf1	heat shock protein-like protein	*Coptotermes formosanus*	0.79	0.03	2.00	0.01	2.52	0.00
Cluster-14773.21772_orf1	heat shock protein 90	*Procambarus clarkii*	0.84	0.13	1.54	0.00	1.83	0.00
Cluster-14773.26606_orf1	protein disulfide isomerase 1	*Fenneropenaeus chinensis*	0.76	0.12	1.85	0.02	2.44	0.01
Cluster-14773.30082_orf1	Translocon-associated protein subunit alpha	*Zootermopsis nevadensis*	0.97	0.88	57.73	0.00	70.16	0.00
Cluster-14773.31479_orf1	heat shock protein 40	*Marsupenaeus japonicus*	1.00	0.97	1.68	0.00	1.68	0.00
Cluster-14773.32162_orf1	hypothetical protein DAPPUDRAFT_194601	*Daphnia pulex*	0.66	0.12	1.51	0.01	2.30	0.00
Cluster-14773.48642_orf1	heat shock protein 21	*Macrobrachium rosenbergii*	0.87	0.50	1.48	0.10	1.69	0.03
Cluster-14773.28305_orf1	protein transport protein Sec61 subunit alpha isoform 2	*Aplysia californica*	1.76	0.00	2.53	0.00	1.44	0.00
Cluster-14773.32900_orf1	conserved hypothetical protein	*Pediculus humanus corporis*	2.88	0.01	4.40	0.01	1.53	0.07
Cluster-14773.29903_orf1	Neutral alpha-glucosidase AB	*Zootermopsis nevadensis*	6.77	0.21	10.08	0.00	1.49	0.45
Cluster-14773.34427_orf1	endoplasmic reticulum oxidoreductin-1 alpha	*Litopenaeus vannamei*	0.81	0.28	0.53	0.03	0.65	0.16
Cluster-14773.43893_orf1	hypothetical protein DAPPUDRAFT_299872	*Daphnia pulex*	0.50	0.11	0.30	0.03	0.61	0.34
Cluster-15601.0_orf1	ubiquitin fusion-degradation protein, putative	*Ixodes scapularis*	0.80	0.78	0.20	0.01	0.24	0.41
Cluster-14773.29777_orf1	dolichyl-diphosphooligosaccharide--protein glycosyltransferase 48 kDa subunit	*Cerapachys biroi*	1.65	0.46	0.09	0.20	0.06	0.04
Cluster-14773.32965_orf1	UDP-glucose:glycoprotein glucosyltransferase	*Tribolium castaneum*	1.32	0.00	0.66	0.08	0.49	0.01
Cluster-14773.39230_orf1	hypothetical protein DAPPUDRAFT_306567	*Daphnia pulex*	1.45	0.07	0.44	0.07	0.31	0.00
Cluster-33501.0_orf1	hypothetical protein BRAFLDRAFT_125408	*Branchiostoma floridae*	1.83	0.00	0.36	0.01	0.20	0.00
Cluster-14773.29530_orf1	hypothetical protein BRAFLDRAFT_85925	*Branchiostoma floridae*	1.29	0.04	0.53	0.02	0.41	0.00
Cluster-14773.29600_orf1	lectin, mannose-binding, 1	*Daphnia pulex*	1.69	0.18	0.19	0.00	0.11	0.02
Cluster-14773.30416_orf1	heat shock protein 90	*Palaemon carinicauda*	0.91	0.66	0.14	0.00	0.16	0.00
Cluster-14773.30964_orf1	S-phase kinase-associated protein 1	*Eriocheir sinensis*	0.91	0.37	0.24	0.00	0.26	0.01
Cluster-14773.30999_orf1	protein disulfide isomerase 2	*Fenneropenaeus chinensis*	0.96	0.76	0.40	0.00	0.42	0.01
Cluster-14773.32451_orf1	protein disulfide isomerase A6	*Penaeus monodon*	1.30	0.03	0.35	0.00	0.27	0.00
Cluster-14773.30275_orf1	endoplasmic reticulum protein 57	*Penaeus monodon*	0.57	0.02	0.16	0.00	0.28	0.00
Metabolism process								
Arginine and proline metabolism								
Cluster-14773.33722_orf1	delta-1-pyrroline-5-carboxylate dehydrogenase, mitochondrial	*Tribolium castaneum*	0.70	0.00	0.65	0.00	0.94	0.21
Cluster-14773.34080_orf1	hypothetical protein CAPTEDRAFT_177352	*Capitella teleta*	0.83	0.20	0.59	0.02	0.71	0.05
Cluster-14773.26949_orf1	hypothetical protein CAPTEDRAFT_179534	*Capitella teleta*	0.49	0.06	0.03	0.01	0.06	0.00
Cluster-14773.27917_orf1	AAEL005289-PA	*Aedes aegypti*	0.93	0.28	0.19	0.00	0.20	0.00
Cluster-14773.33238_orf1	hypothetical protein DAPPUDRAFT_51170	*Daphnia pulex*	0.67	0.03	0.31	0.00	0.46	0.01
Cluster-14773.35801_orf1	spermidine synthase	*Anolis carolinensis*	0.76	0.30	0.25	0.02	0.33	0.01
Cluster-14773.30732_orf1	arginine kinase	*Litopenaeus vannamei*	0.76	0.02	0.17	0.00	0.22	0.00
Tyrosine metabolism								
Cluster-14773.33092_orf1	hemocyanin	*Fenneropenaeus chinensis*	0.40	0.06	0.11	0.00	0.28	0.27
Cluster-14773.22076_orf1	hemocyanin	*Fenneropenaeus chinensis*	1.14	0.37	0.29	0.00	0.25	0.00
Cluster-14773.30500_orf1	hemocyanin subunit L3	*Litopenaeus vannamei*	0.81	0.02	0.08	0.00	0.10	0.00
Cluster-14773.30709_orf1	hemocyanin subunit L2	*Litopenaeus vannamei*	1.06	0.59	0.11	0.00	0.11	0.00
Cluster-14773.30853_orf1	hemocyanin	*Litopenaeus vannamei*	0.95	0.28	0.34	0.00	0.35	0.00
Cluster-14773.30881_orf1	hemocyanin subunit L1	*Litopenaeus vannamei*	0.90	0.02	0.14	0.00	0.15	0.00
Cluster-14773.30960_orf1	hemocyanin subunit L2	*Litopenaeus vannamei*	0.87	0.03	0.13	0.00	0.14	0.00
Cluster-14773.7946_orf1	hemocyanin subunit L5	*Litopenaeus vannamei*	0.82	0.01	0.40	0.00	0.49	0.00
Glutathione metabolism								
Cluster-14773.32282_orf1	putative aminopeptidase W07G4.4-like	*Latimeria chalumnae*	0.76	0.37	0.58	0.03	0.76	0.46
Cluster-14773.39596_orf1	glutathione S-transferase	*Palaemon carinicauda*	0.98	0.95	0.09	0.00	0.09	0.07
Cluster-14773.33698_orf1	aminopeptidase N-like	*Nasonia vitripennis*	1.81	0.04	0.29	0.05	0.16	0.00
Cluster-14773.35801_orf1	spermidine synthase	*Anolis carolinensis*	0.76	0.30	0.25	0.02	0.33	0.01
Cluster-14773.32166_orf1	6-phosphogluconate dehydrogenase, decarboxylating isoform X1	*Strongylocentrotus purpuratus*	0.68	0.07	0.32	0.01	0.46	0.00
Cluster-14773.23606_orf1	hypothetical protein DAPPUDRAFT_304194	*Daphnia pulex*	1.13	0.11	0.10	0.00	0.08	0.00
Glycerolipid metabolism/ Histidine metabolism								
Cluster-14773.34080_orf1	hypothetical protein CAPTEDRAFT_177352	*Capitella teleta*	0.83	0.20	0.59	0.02	0.71	0.05
Cluster-14773.26949_orf1	hypothetical protein CAPTEDRAFT_179534	*Capitella teleta*	0.49	0.06	0.03	0.01	0.06	0.00
Cluster-14773.33238_orf1	hypothetical protein DAPPUDRAFT_51170	*Daphnia pulex*	0.67	0.03	0.31	0.00	0.46	0.01
Cysteine and methionine metabolism								
Cluster-14773.32551_orf1	hypothetical protein DAPPUDRAFT_300660	*Daphnia pulex*	1.68	0.11	0.84	0.32	0.50	0.05
Cluster-14773.35801_orf1	spermidine synthase	*Anolis carolinensis*	0.76	0.30	0.25	0.02	0.33	0.01
Cluster-14773.28965_orf1	lactate dehydrogenase	*Litopenaeus vannamei*	0.89	0.21	0.09	0.00	0.10	0.00
Cluster-14773.29677_orf1	putative adenosylhomocysteinase 2 isoform X1	*Pogonomyrmex barbatus*	0.76	0.03	0.16	0.00	0.21	0.00
Cluster-14773.29915_orf1	Adenosylhomocysteinase A	*Stegodyphus mimosarum*	0.82	0.12	0.30	0.00	0.37	0.00
Cluster-14773.30482_orf1	Kynurenine--oxoglutarate transaminase 3	*Zootermopsis nevadensis*	0.99	0.83	0.35	0.00	0.35	0.00
Cluster-14773.33044_orf1	hypothetical protein DAPPUDRAFT_306997	*Daphnia pulex*	0.93	0.41	0.12	0.00	0.13	0.00

(*continued on next page*)

Table 3 (*continued*)

Fatty acid metabolism								
Cluster-14773.31075_orf1	non-specific lipid-transfer protein	*Athalia rosae*	**1.89**	0.28	**5.65**	0.00	**2.99**	0.00
Cluster-14773.21680_orf1	long-chain-fatty-acid--CoA ligase 4	*Microplitis demolitor*	**0.90**	0.45	**0.60**	0.04	0.67	0.02
Cluster-14773.31112_orf1	hypothetical protein DAPPUDRAFT_58917	*Daphnia pulex*	**1.33**	0.49	0.14	0.12	**0.11**	0.00
Cluster-14773.35101_orf1	hypothetical protein DAPPUDRAFT_302851	*Daphnia pulex*	**1.39**	0.49	0.32	0.21	**0.23**	0.01
Carbon metabolism								
Cluster-14773.31327_orf1	hypothetical protein L798_14210	*Zootermopsis nevadensis*	**1.54**	0.03	**1.74**	0.01	1.13	0.41
Cluster-14773.33345_orf1	alanine aminotransferase	*Leptinotarsa decemlineata*	**0.53**	0.11	**0.06**	0.00	0.11	0.09
Cluster-14773.28005_orf1	probable pyruvate dehydrogenase E1 component subunit alpha, mitochondrial	*Solenopsis invicta*	**0.34**	0.04	**0.23**	0.02	0.69	0.45
Cluster-14773.33303_orf1	triose-phosphate isomerase	*Litopenaeus vannamei*	**0.03**	0.00	**0.22**	0.02	7.32	0.33
Cluster-24630.0_orf1	triosephosphate isomerase	*Obelia sp. KJP-2004*	**0.35**	0.02	**0.22**	0.00	0.63	0.51
Cluster-14773.30513_orf1	Phosphoglycerate mutase 2	*Zootermopsis nevadensis*	**0.89**	0.61	0.59	0.12	**0.66**	0.05
Cluster-14773.30660_orf1	putative phosphoglycerate kinase	*Danaus plexippus*	**1.83**	0.26	0.58	0.54	**0.32**	0.00
Cluster-14773.31213_orf1	hypothetical protein ZHAS_00018295	*Anopheles sinensis*	**1.06**	0.37	0.67	0.02	**0.63**	0.00
Cluster-14773.31351_orf1	glutamate dehydrogenase	*Litopenaeus vannamei*	**1.24**	0.05	0.81	0.03	**0.66**	0.00
Cluster-28467.0_orf1	probable phosphoglycerate kinase	*Hydra vulgaris*	**0.79**	0.76	0.27	0.32	**0.34**	0.04
Cluster-14773.32166_orf1	6-phosphogluconate dehydrogenase, decarboxylating isoform X1	*Strongylocentrotus purpuratus*	**0.68**	0.07	**0.32**	0.01	**0.46**	0.00
Cluster-14773.30608_orf1	glyceraldehyde-3-phosphate-dehydrogenase	*Cherax cainii*	**1.01**	0.90	**0.59**	0.04	**0.58**	0.02
Cluster-14773.31873_orf1	Pyruvate dehydrogenase E1 component subunit beta, mitochondrial	*Zootermopsis nevadensis*	**1.07**	0.72	**0.27**	0.02	**0.26**	0.00
Cluster-14773.32520_orf1	putative isocitrate dehydrogenase subunit beta, mitochondrial	*Zootermopsis nevadensis*	**0.99**	0.83	**0.40**	0.02	**0.40**	0.02
Cluster-14773.44098_orf1	phosphoglycolate phosphatase	*Tribolium castaneum*	**1.15**	0.16	**0.13**	0.00	**0.11**	0.00
Cell adhesion process								
Focal adhesion								
Cluster-14773.28604_orf1	uncharacterized protein LOC100159331 isoform X2	*Acyrthosiphon pisum*	**0.81**	0.71	**1.93**	0.04	**2.38**	0.04
Cluster-14773.31771_orf1	putative myosin regulatory light chain 2 smooth muscle	*Scylla paramamosain*	**0.65**	0.01	**1.17**	0.05	**1.80**	0.00
Cluster-14773.11824_orf1	Laminin subunit beta-1	*Zootermopsis nevadensis*	**2.74**	0.01	**1.96**	0.04	**0.72**	0.01
Cluster-14773.37452_orf1	hypothetical protein DAPPUDRAFT_60396	*Daphnia pulex*	**2.14**	0.00	**3.12**	0.00	**1.45**	0.01
Cluster-41437.0_orf1	actin-1, putative	*Acanthamoeba castellanii str. Neff*	**1.47**	0.11	**1.99**	0.02	**1.35**	0.18
Cluster-41659.1_orf1	hypothetical protein DAPPUDRAFT_321711	*Daphnia pulex*	**1.64**	0.01	**1.41**	0.01	**0.86**	0.16
Cluster-14773.23301_orf1	Filamin-C, putative	*Pediculus humanus corporis*	**0.72**	0.07	**0.49**	0.01	**0.68**	0.02
Cluster-14773.41998_orf1	beta actin	*Aurelia aurita*	**2.11**	0.00	**1.08**	0.74	**0.51**	0.01
Cluster-43580.1_orf1	Laminin subunit alpha	*Zootermopsis nevadensis*	**1.75**	0.02	**1.10**	0.66	**0.63**	0.01
Cluster-14773.30747_orf1	actin	*Penaeus monodon*	**1.88**	0.01	**0.69**	0.04	**0.37**	0.04
Cluster-14773.36449_orf1	hypothetical protein L798_12707	*Zootermopsis nevadensis*	**0.82**	0.52	**0.41**	0.06	**0.50**	0.04
Cluster-14773.47749_orf1	Thrombospondin-3 precursor, putative	*Pediculus humanus corporis*	**1.75**	0.06	**0.65**	0.19	**0.37**	0.01
Cluster-14773.29589_orf1	Cdc42	*Litopenaeus vannamei*	**0.82**	0.26	**0.19**	0.00	**0.24**	0.01
Cluster-14773.32054_orf1	filamin-A isoform X3	*Tribolium castaneum*	**1.10**	0.58	**0.63**	0.01	**0.57**	0.04
Cluster-18309.0_orf1	ras-related C3 botulinum toxin substrate 1	*Dipodomys ordii*	**0.81**	0.09	**0.44**	0.00	**0.55**	0.00
Cluster-31172.1_orf1	rho-related GTP-binding protein RhoC	*Danio rerio*	**0.66**	0.09	**0.19**	0.00	**0.29**	0.00
Tight junction								
Cluster-14773.31639_orf1	afadin isoform X2	*Orussus abietinus*	**1.19**	0.13	**1.81**	0.00	**1.52**	0.02
Cluster-14773.33948_orf1	Src substrate cortactin	*Zootermopsis nevadensis*	**1.08**	0.59	**1.64**	0.02	**1.52**	0.04
Cluster-14773.31771_orf1	putative myosin regulatory light chain 2 smooth muscle	*Scylla paramamosain*	**0.65**	0.01	**1.17**	0.05	**1.80**	0.00
Cluster-14773.30313_orf1	alpha-tubulin	*Eriocheir sinensis*	**1.67**	0.00	**1.61**	0.00	**0.97**	0.68
Cluster-14773.33555_orf1	hypothetical protein DAPPUDRAFT_327006	*Daphnia pulex*	**2.18**	0.00	**3.01**	0.00	**1.38**	0.01
Cluster-41437.0_orf1	actin-1, putative	*Acanthamoeba castellanii str. Neff*	**1.47**	0.11	**1.99**	0.02	**1.35**	0.18
Cluster-14773.30376_orf1	myosin essential light chain	*Eriocheir sinensis*	**0.70**	0.09	**0.47**	0.01	**0.67**	0.06
Cluster-14773.41998_orf1	beta actin	*Aurelia aurita*	**2.11**	0.00	**1.08**	0.74	**0.51**	0.01
Cluster-14773.30747_orf1	actin	*Penaeus monodon*	**1.88**	0.01	**0.69**	0.04	**0.37**	0.04
Cluster-14773.32147_orf1	proliferating cell nuclear antigen	*Litopenaeus vannamei*	**3.61**	0.07	**0.28**	0.48	**0.08**	0.00
Cluster-14773.34525_orf1	AMP-activated protein kinase subunit gamma	*Litopenaeus vannamei*	**1.54**	0.27	**0.35**	0.21	**0.23**	0.01
Cluster-14773.26708_orf1	lethal(2) giant larvae protein homolog 1 isoform X3	*Athalia rosae*	**0.78**	0.02	**0.35**	0.00	**0.45**	0.00
Cluster-14773.29589_orf1	Cdc42	*Litopenaeus vannamei*	**0.82**	0.26	**0.19**	0.00	**0.24**	0.01
Cluster-14773.30262_orf1	actin	*Cryptocercus punctulatus*	**1.39**	0.02	**0.64**	0.01	**0.46**	0.00
Cluster-14773.30707_orf1	myosin heavy chain, non-muscle isoform X1	*Bombus impatiens*	**0.79**	0.00	**0.42**	0.00	**0.53**	0.00
Cluster-14773.3071_orf1	tubulin alpha-1B chain-like	*Xiphophorus maculatus*	**0.70**	0.07	**0.15**	0.00	**0.21**	0.00
Cluster-14773.31109_orf1	alpha-III tubulin	*Homarus americanus*	**1.30**	0.16	**0.55**	0.00	**0.42**	0.01
Cluster-14773.38778_orf1	hypothetical protein DAPPUDRAFT_301963	*Daphnia pulex*	**0.76**	0.12	**0.05**	0.00	**0.07**	0.00
Cluster-18309.0_orf1	ras-related C3 botulinum toxin substrate 1	*Dipodomys ordii*	**0.81**	0.09	**0.44**	0.00	**0.55**	0.00
Cluster-14773.38776_orf1	protein kinase C-like	*Plutella xylostella*	**0.58**	0.00	**0.24**	0.00	**0.42**	0.00
Cluster-31172.1_orf1	rho-related GTP-binding protein RhoC	*Danio rerio*	**0.66**	0.09	**0.19**	0.00	**0.29**	0.00
ECM-receptor interaction								
Cluster-14773.29642_orf1	integrin	*Litopenaeus vannamei*	**1.52**	0.05	**1.44**	0.03	**0.95**	0.61
Cluster-14773.30290_orf1	Collagen alpha-2(I) chain	*Zootermopsis nevadensis*	**1.97**	0.04	**4.04**	0.00	**2.05**	0.00
Cluster-14773.11824_orf1	Laminin subunit beta-1	*Zootermopsis nevadensis*	**2.74**	0.01	**1.96**	0.04	**0.72**	0.01
Cluster-14773.28273_orf1	hypothetical protein DAPPUDRAFT_232498	*Daphnia pulex*	**2.56**	0.00	**3.02**	0.00	**1.18**	0.05
Cluster-14773.37452_orf1	hypothetical protein DAPPUDRAFT_60396	*Daphnia pulex*	**2.14**	0.00	**3.12**	0.00	**1.45**	0.01
Cluster-41659.1_orf1	hypothetical protein DAPPUDRAFT_321711	*Daphnia pulex*	**1.64**	0.01	**1.41**	0.01	**0.86**	0.16
Cluster-43580.1_orf1	Laminin subunit alpha	*Zootermopsis nevadensis*	**1.75**	0.02	**1.10**	0.66	**0.63**	0.01
Cluster-14773.34686_orf1	Basement membrane-specific heparan sulfate proteoglycan core protein	*Zootermopsis nevadensis*	**1.04**	0.96	**3.08**	0.02	**2.98**	0.02
Cluster-35625.0_orf1	collagen alpha chain, type IV, putative	*Pediculus humanus corporis*	**0.98**	0.94	**0.39**	0.00	**0.40**	0.06
Cluster-14773.18441_orf1	Basement membrane-specific heparan sulfate proteoglycan core protein	*Zootermopsis nevadensis*	**0.68**	0.26	**0.32**	0.05	**0.47**	0.00
Cluster-14773.47749_orf1	Thrombospondin-3 precursor, putative	*Pediculus humanus corporis*	**1.75**	0.06	**0.65**	0.19	**0.37**	0.01
Cluster-14773.37981_orf1	Collagen alpha-1(XI) chain	*Zootermopsis nevadensis*	**1.01**	0.94	**0.23**	0.00	**0.23**	0.00
Cell signaling process								
Calcium signaling pathway								
Cluster-14773.28604_orf1	uncharacterized protein LOC100159331 isoform X2	*Acyrthosiphon pisum*	**0.81**	0.71	**1.93**	0.04	**2.38**	0.04
Cluster-14773.31217_orf1	adenine nucleotide translocase 2	*Litopenaeus vannamei*	**2.83**	0.00	**4.65**	0.00	**1.64**	0.01
Cluster-14773.30161_orf1	sarco/endoplasmic reticulum Ca2+-ATPase	*Litopenaeus vannamei*	**1.37**	0.00	**1.70**	0.00	**1.24**	0.05
Cluster-14773.31653_orf1	calcium/calmodulin-dependent protein kinase II isoform A	*Periplaneta americana*	**1.94**	0.02	**1.53**	0.01	**0.79**	0.17
Cluster-14773.37975_orf1	plasma membrane calcium ATPase	*Callinectes sapidus*	**1.49**	0.00	**1.69**	0.00	**1.14**	0.09
Cluster-14773.30769_orf1	calmodulin-A-like	*Callorhinchus milii*	**1.24**	0.02	**0.69**	0.00	**0.56**	0.00

(*continued on next page*)

Table 3 (*continued*)

Cluster-14773.32218_orf1	G protein s alpha subunit	*Litopenaeus vannamei*	2.07	0.00	1.18	0.51	0.57	0.01
Cluster-14773.32473_orf1	calcium-transporting ATPase	*Cherax cainii*	2.14	0.08	0.08	0.11	0.04	0.00
Cluster-14773.32090_orf1	voltage-dependent anion-selective channel	*Eriocheir sinensis*	0.60	0.00	0.21	0.00	0.35	0.00
Cluster-14773.34005_orf1	GTP binding protein alpha subunit Gq	*Marsupenaeus japonicus*	0.95	0.62	0.27	0.00	0.28	0.00
Cluster-14773.37908_orf1	1-phosphatidylinositol-4,5-bisphosphate phosphodiesterase delta-4	*Zootermopsis nevadensis*	0.59	0.01	0.27	0.00	0.45	0.02
Oxytocin signaling pathway								
Cluster-14773.28604_orf1	uncharacterized protein LOC100159331 isoform X2	*Acyrthosiphon pisum*	0.81	0.71	1.93	0.04	2.38	0.04
Cluster-14773.31653_orf1	calcium/calmodulin-dependent protein kinase II isoform A	*Periplaneta americana*	1.94	0.02	1.53	0.01	0.79	0.17
Cluster-41437.0_orf1	actin-1, putative	*Acanthamoeba castellanii str. Neff*	1.47	0.11	1.99	0.02	1.35	0.18
Cluster-14773.23252_orf1	calcium-calmodulin dependent protein kinase I	*Macrobrachium nipponense*	1.66	0.02	0.83	0.60	0.50	0.05
Cluster-14773.30376_orf1	myosin essential light chain	*Eriocheir sinensis*	0.70	0.09	0.47	0.01	0.67	0.06
Cluster-14773.32218_orf1	G protein s alpha subunit	*Litopenaeus vannamei*	2.07	0.00	1.18	0.51	0.57	0.01
Cluster-14773.41998_orf1	beta actin	*Aurelia aurita*	2.11	0.00	1.08	0.74	0.51	0.01
Cluster-14773.30769_orf1	calmodulin-A-like	*Callorhinchus milii*	1.24	0.02	0.69	0.00	0.56	0.00
Cluster-14773.30747_orf1	actin	*Penaeus monodon*	1.88	0.01	0.69	0.04	0.37	0.04
Cluster-14773.34525_orf1	AMP-activated protein kinase subunit gamma	*Litopenaeus vannamei*	1.54	0.27	0.35	0.21	0.23	0.01
Cluster-14773.34005_orf1	GTP binding protein alpha subunit Gq	*Marsupenaeus japonicus*	0.95	0.62	0.27	0.00	0.28	0.00
Cluster-14773.30553_orf1	elongation factor 2	*Litopenaeus vannamei*	1.22	0.14	0.40	0.00	0.33	0.00
Cluster-31172.1_orf1	rho-related GTP-binding protein RhoC	*Danio rerio*	0.66	0.09	0.19	0.00	0.29	0.00
FoxO signaling pathway								
Cluster-14773.28046_orf1	mitochondrial MnSOD	*Litopenaeus vannamei*	0.86	0.09	0.16	0.00	0.19	0.00
Cluster-14773.28735_orf1	protein arginine N-methyltransferase 1 isoform X1	*Athalia rosae*	1.77	0.00	2.59	0.00	1.47	0.00
Cluster-14773.30205_orf1	cytosolic MnSOD	*Litopenaeus vannamei*	0.57	0.00	0.31	0.00	0.55	0.00
Cluster-14773.32118_orf1	Ubiquitin carboxyl-terminal hydrolase 7	*Zootermopsis nevadensis*	0.57	0.41	2.02	0.00	3.53	0.04
Wnt signaling pathway								
Cluster-14773.22091_orf1	c-jun N-terminal kinase	*Marsupenaeus japonicus*	0.79	0.03	0.70	0.03	0.89	0.46
Cluster-14773.36711_orf1	Segment polarity protein dishevelled-like protein DVL-3	*Zootermopsis nevadensis*	1.04	0.93	0.48	0.22	0.47	0.09
Cluster-14773.30964_orf1	S-phase kinase-associated protein 1	*Eriocheir sinensis*	0.91	0.37	0.24	0.00	0.26	0.01
Cluster-14773.34168_orf1	testin isoform X1	*Takifugu rubripes*	0.64	0.33	0.35	0.01	0.54	0.40
Cluster-18309.0_orf1	ras-related C3 botulinum toxin substrate 1	*Dipodomys ordii*	0.81	0.09	0.44	0.00	0.55	0.00
Cluster-31172.1_orf1	rho-related GTP-binding protein RhoC	*Danio rerio*	0.66	0.09	0.19	0.00	0.29	0.00

Red shade represent protein was significantly up-regulation, green shade represent protein was significantly down-regulation.

metabolism, methylamines and SCFAs [37]. In the present study, we found that some proteins involved in carbohydrate metabolic processes were significantly upregulated after shrimp were fed normal HC-2, but proteins participated in other metabolic pathways, including arginine and proline, tyrosine, glutathione, glycerolipid/histidine, cysteine and methionine. Fatty acid metabolism was insignificant. However, feeding with LiCl-treated HC-2 led to the overall downregulation of these metabolism-related proteins, which indicated that surface proteins are important in HC-2 regulation and the maintenance of shrimp intestinal metabolism. Adhesion is the interaction of the bacterial surface structure (adhesin) attached to the surface receptors on the epithelial cells of the host, the first step of bacterial colonization and is the key for bacteria to grow, reproduce and function. Recent studies have indicated that the attachment of bacteria, including the hydrophobicity and self-agglutination of the bacterial surface, lipoteichoic acid (LTA), exopolysaccharides (EPS) and cell surface proteins related to mucosal surfaces, is the initial event in intestinal adhesion and colonization [16,38]. In addition, many surface proteins that mediate adhesion in lactobacillus have been reported, such as CmbA/Lar_0958, EF-Tu, GAPDH, GroEL, Lam 29, MapA, MBF, Msa, Mub (Mub family), Pili, 32-Mmubp, FbpA and GroEL [39–41]. Probiotics adhere to host intestinal mucus, intestinal epithelial cells, and extracellular stroma by means of

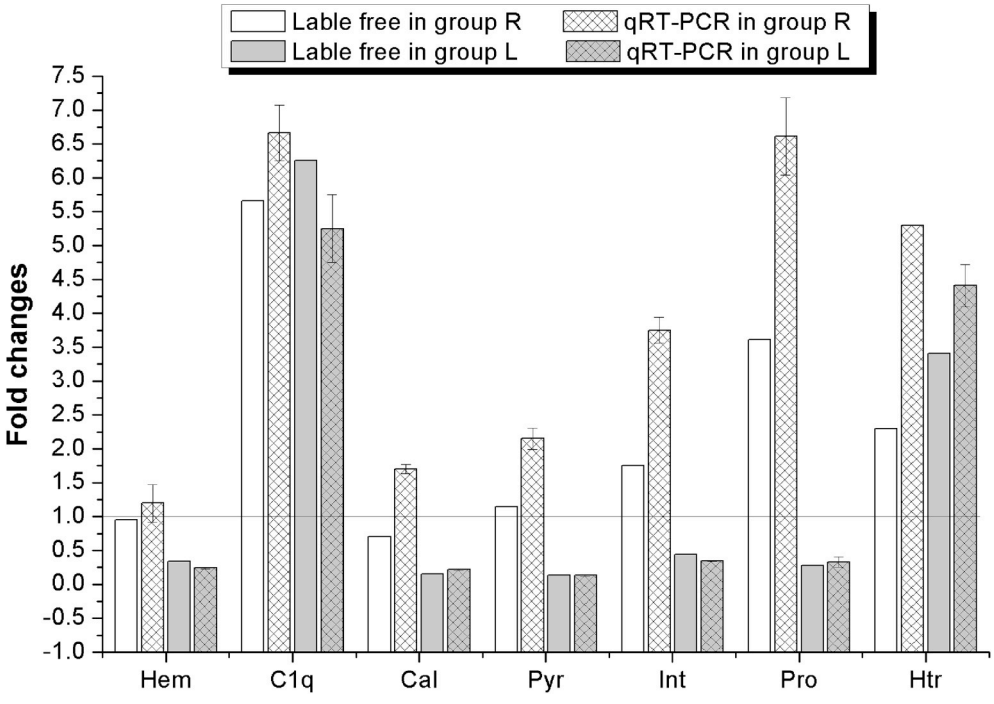

Fig. 7. Validation analysis of label-free proteomics using quantitative real-time PCR to determine the selected protein expression in the midgut of *L. vannamei*. Note: R, shrimp were fed a basal diet supplemented with normal *L. pentosus* HC-2; L, shrimp were fed a basal diet supplemented with LiCl-treated *L. pentosus* HC-2. Fold changes in protein expression represent the experimental groups compared with the control group.

its surface proteins, and/or other bacteria and lipodermoid acid to effectively prevent pathogen infections [42–44]. In the present study, many related cell-adhesion proteins were significantly upregulated in the shrimp midgut after feeding with normal HC-2, but LiCl-treated HC-2 induced significant downregulation of many cell-adhesion proteins. In addition to adhesion ability, surface proteins have important functions in cell-cell signaling processes and interactions with the host immune system or environment [45]. In this study, we found that the proteins involved in the cell-cell-signaling pathway were upregulated in the shrimp midgut after feeding with normal HC-2, but after feeding with surface proteins, shaving bacteria induced these proteins to decrease. These results indicated that surface proteins play a crucial role in the adhesion and colonization of HC-2 in the shrimp midgut and contributed to the activation of a series of molecular signal communications with the surface cell of the host.

5. Conclusion

To summarize, feeding normal HC-2 obviously improved the intestinal histology and enhanced the protective effect against pathogen damage, but feeding LiCl-treated HC-2 did not improve the intestinal structure. GO and KEGG enrichment analyses of significant proteins in the R/control and L/control indicated that most proteins were involved in immune system processes, metabolic processes, adhesion processes, and cell-cell-signaling processes. However, these proteins were significantly upregulated in the shrimp midgut after feeding normal HC-2 and were significantly downregulated in shrimp fed LiCl-treated HC-2. The results of the present work indicated that surface proteins play an important role in the mediation of HC-2 to improve intestinal histology, immune response, metabolic, adhesion and signaling communication in the midgut of shrimp, which might provide base data to understand the probiotic mechanism excised by HC-2.

Acknowledgments

This research was supported by the National Natural Science Foundation of China (41906107), the China Postdoctoral Science Foundation (2018M632736), and the Scientific and technological development fund project of Shinan district of Qingdao city (2018-4-001-ZH). We are grateful to all the laboratory members for their technical advice and helpful suggestions.

Appendix A. Supplementary data

Supplementary data to this article can be found online at https://doi.org/10.1016/j.fsi.2019.10.059.

References

[1] P.F. Ji, C.L. Yao, Z.Y. Wang, Two types of calmodulin play different roles in Pacific white shrimp (*Litopenaeus vannamei*) defenses against *Vibrio parahaemolyticus* and WSSV infection, Fish Shellfish Immunol. 31 (2011) 260–268.
[2] D.V. Lightner, Virus diseases of farmed shrimp in the Western Hemisphere (the Americas): a review, J. Invertebr. Pathol. 106 (2011) 110–130.
[3] F. Li, J. Xiang, Signaling pathways regulating innate immune responses in shrimp, Fish Shellfish Immunol. 34 (2013) 973–980.
[4] L. Verschuere, G. Rombaut, P. Sorgeloos, W. Verstraete, Probiotic bacteria as biological control agents in aquaculture, Microbiol. Mol. Biol. Rev. 64 (2000) 655–671.
[5] M.A.O. Dawood, S. Koshio, M.M. Abdel-Daim, H. Van Doan, Probiotic application for sustainable aquaculture, Rev. Aquac. (2018) 1–18.
[6] M. Yousefian, M.S. Amiri, A review of the use of prebiotic in aquaculture for fish and shrimp, Afr. J. Biotechnol. 8 (2009) 7313–7318.
[7] B.A. Ige, Probiotics use in intensive fish farming, Afr. J. Microbiol. Res. 7 (2013) 2701–2711.
[8] M. Maeda, A. Shibata, G. Biswas, H. Korenaga, T. Kono, T. Itami, et al., Isolation of lactic acid bacteria from kuruma shrimp (*Marsupenaeus japonicus*) intestine and assessment of immunomodulatory role of a selected strain as probiotic, Mar. Biotechnol. 16 (2014) 181–192.
[9] A. Kesarcodi-Watson, H. Kaspar, M.J. Lategan, L. Gibson, Probiotics in aquaculture: the need, principles and mechanisms of action and screening processes, Aquaculture 274 (2008) 1–14.
[10] C. Heinemann, J.E.T. van Hylckama Vlieg, D.B. Janssen, H.J. Busscher, H.C. van der Mei, G. Reid, Purification and characterization of a surface-binding protein from *Lactobacillus fermentum* RC-14 that inhibits adhesion of *Enterococcus faecalis* 1131, FEMS Microbiol. Lett. 190 (2000) 177–180.
[11] M. Rojas, F. Ascencio, P.L. Conway, Purification and characterization of a surface protein from Lactobacillus fermentum 104R that binds to porcine small intestinal mucus and gastric mucin, Appl. Environ. Microbiol. 68 (2002) 2330–2336.
[12] S. Roos, H. Jonsson, A high-molecular-mass cell-surface protein from *Lactobacillus reuteri* 1063 adheres to mucus components, Microbiology 148 (2002) 433–442.
[13] M. Jakava-Viljanen, A. Palva, Isolation of surface (S) layer protein carrying Lactobacillus species from porcine intestine and faeces and characterization of their adhesion properties to different host tissues, Vet. Microbiol. 124 (2007) 264–273.
[14] X. Chen, J. Xu, J. Shuai, J. Chen, Z. Zhang, W. Fang, The S-layer proteins of *Lactobacillus crispatus* strain ZJ001 is responsible for competitive exclusion against Escherichia coli O157: H7 and Salmonella typhimurium, Int. J. Food Microbiol. 115 (2007) 307–312.
[15] S.R. Konstantinov, H. Smidt, W.M. De Vos, S.C.M. Bruijns, S.K. Singh, F. Valence, et al., S layer protein A of *Lactobacillus acidophilus* NCFM regulates immature dendritic cell and T cell functions, Proc. Natl. Acad. Sci. 105 (2008) 19474–19479.
[16] B. Kos, J. Šušković, S. Vuković, M. Šimpraga, J. Frece, S. Matošić, Adhesion and aggregation ability of probiotic strain Lactobacillus acidophilus M92, J. Appl. Microbiol. 94 (2003) 981–987.
[17] H.C. der Mei, B. de Belt-Gritter, P.H. Pouwels, B. Martinez, H.J. Busscher, Cell surface hydrophobicity is conveyed by S-layer proteins-a study in recombinant lactobacilli, Colloids Surfaces B Biointerfaces 28 (2003) 127–134.
[18] E. Smit, F. Oling, R. Demel, B. Martinez, P.H. Pouwels, The S-layer protein of *Lactobacillus acidophilus* ATCC 4356: identification and characterisation of domains responsible for S-protein assembly and cell wall binding, J. Mol. Biol. 305 (2001) 245–257.
[19] Y. Sha, B. Wang, M. Liu, K. Jiang, L. Wang, Interaction between *Lactobacillus pentosus* HC-2 and *Vibrio parahaemolyticus* E1 in *Litopenaeus vannamei* in vivo and in vitro, Aquaculture 465 (2016) 17–123.
[20] Y. Sha, M. Liu, B. Wang, K. Jiang, C. Qi, L. Wang, Bacterial population in intestines of *litopenaeus vannamei* fed different probiotics or probiotic supernatant, J. Microbiol. Biotechnol. 26 (2016) 1736–1745.
[21] Y. Sha, L. Wang, M. Liu, K. Jiang, F. Xin, B. Wang, Effects of lactic acid bacteria and the corresponding supernatant on the survival, growth performance, immune response and disease resistance of *Litopenaeus vannamei*, Aquaculture 452 (2016) 28–36.
[22] Y. Du, S. Zhou, M. Liu, B. Wang, K. Jiang, H. Fang, L. Wang, Understanding the roles of surface proteins in regulation of *Lactobacillus pentosus* HC-2 to immune response and bacterial diversity in midgut of *Litopenaeus vannamei*, Fish Shellfish Immunol. 86 (2019) 1194–1206.
[23] D. Sengupta, M. Kannan, A.R. Reddy, A root proteomics-based insight reveals dynamic regulation of root proteins under progressive drought stress and recovery in *Vigna radiata* (L.) Wilczek, Planta 233 (2011) 1111–1127.
[24] M.M. Bradford, A rapid and sensitive method for the quantitation of microgram quantities of protein utilizing the principle of protein-dye binding, Anal. Biochem. 72 (1976) 248–254.
[25] J. Cox, A. Michalski, M. Mann, Software lock mass by two-dimensional minimization of peptide mass errors, J. Am. Soc. Mass Spectrom. 22 (2011) 1373–1380.
[26] C.A. Luber, J. Cox, H. Lauterbach, B. Fancke, M. Selbach, J. Tschopp, et al., Quantitative proteomics reveals subset-specific viral recognition in dendritic cells, Immunity 32 (2010) 279–289.
[27] G.O. Consortium, The Gene Ontology (GO) database and informatics resource, Nucleic Acids Res. 32 (2004) 258–261.
[28] E. Cardona, Y. Gueguen, K. Magré, B. Lorgeoux, D. Piquemal, F. Pierrat, et al., Bacterial community characterization of water and intestine of the shrimp *Litopenaeus stylirostris* in a biofloc system, BMC Microbiol. 16 (2016) 1–9.
[29] M. Lara-Flores, The use of probiotic in aquaculture: an overview, Int. Res. J. Microbiol. 2 (2011) 471–478.
[30] C.L. Daniels, D.L. Merrifield, D.P. Boothroyd, S.J. Davies, J.R. Factor, K.E. Arnold, Effect of dietary Bacillus spp. and mannan oligosaccharides (MOS) on European lobster (*Homarus gammarus* L.) larvae growth performance, gut morphology and gut microbiota, Aquaculture 304 (2010) 49–57.
[31] P. Li, G.S. Burr, D.M. Gatlin, M.E. Hume, S. Patnaik, F.L. Castille, et al., Dietary supplementation of short-chain fructooligosaccharides influences gastrointestinal microbiota composition and immunity characteristics of Pacific white shrimp, *Litopenaeus vannamei*, cultured in a recirculating system, J. Nutr. 137 (2007) 2763–2768.
[32] M.A. de Rodrigáñez, P. Diaz-Rosales, M. Chabrillón, H. Smidt, S. Arijo, J.M. León-Rubio, et al., Effect of dietary administration of probiotics on growth and intestine functionality of juvenile Senegalese sole (Solea senegalensis, Kaup 1858), Aquacult. Nutr. 15 (2009) 177–185.
[33] D.L. Merrifield, G.M. Harper, A. Dimitroglou, E. Ringø, S.J. Davies, Possible influence of probiotic adhesion to intestinal mucosa on the activity and morphology of rainbow trout (*Oncorhynchus mykiss*) enterocytes, Aquacult. Res. 41 (2010) 1268–1272.
[34] G. Wang, Y. Huang, Y. Zhou, S. Dong, W. Huang, Q. Yan, et al., Effects of Lactobacillus on growth performance, digestive enzyme activities and non-specific immunity of *Litopenaeus vannamei*, Chinese J. Anim. Nutr. 22 (2010) 228–234.
[35] C.N. Zheng, W. Wang, Effects of *Lactobacillus pentosus* on the growth performance, digestive enzyme and disease resistance of white shrimp, *Litopenaeus vannamei* (Boone, 1931), Aquacult. Res. 48 (2017) 2767–2777.
[36] S. Lebeer, J. Vanderleyden, S.C.J. De Keersmaecker, Genes and molecules of lactobacilli supporting probiotic action, Microbiol. Mol. Biol. Rev. 72 (2008) 728–764.

[37] F.P.J. Martin, Y. Wang, N. Sprenger, I.K.S. Yap, T. Lundstedt, P. Lek, et al., Probiotic modulation of symbiotic gut microbial-host metabolic interactions in a humanized microbiome mouse model, Mol. Syst. Biol. 4 (2008) 157.
[38] D. Granato, F. Perotti, I. Masserey, M. Rouvet, M. Golliard, A. Servin, et al., Cell surface-associated lipoteichoic acid acts as an adhesion factor for attachment of Lactobacillus johnsonii La1 to human enterocyte-like Caco-2 cells, Appl. Environ. Microbiol. 65 (1999) 1071–1077.
[39] K. Nishiyama, M. Sugiyama, T. Mukai, Adhesion properties of lactic acid bacteria on intestinal mucin, Microorganisms 4 (2016) 1–18.
[40] B.L. Buck, E. Altermann, T. Svingerud, T.R. Klaenhammer, Functional analysis of putative adhesion factors in *Lactobacillus acidophilus* NCFM, Appl. Environ. Microbiol. 71 (2005) 8344–8351.
[41] G.E. Bergonzelli, D. Granato, R.D. Pridmore, L.F. Marvin-Guy, D. Donnicola, I.E. Corthésy-Theulaz, GroEL of *Lactobacillus johnsonii* La1 (NCC 533) is cell surface associated: potential role in interactions with the host and the gastric pathogen Helicobacter pylori, Infect. Immun. 74 (2006) 425–434.
[42] U. Hynönen, B. Westerlund-Wikström, A. Palva, T.K. Korhonen, Identification by flagellum display of an epithelial cell-and fibronectin-binding function in the SlpA surface protein of Lactobacillus brevis, J. Bacteriol. 184 (2002) 3360–3367.
[43] K.C. Johnson-Henry, K.E. Hagen, M. Gordonpour, T.A. Tompkins, P.M. Sherman, Surface-layer protein extracts from Lactobacillus helveticus inhibit enterohaemorrhagic *Escherichia coli* O157: H7 adhesion to epithelial cells, Cell Microbiol. 9 (2007) 356–367.
[44] J. Antikainen, L. Anton, J. Sillanpää, T.K. Korhonen, Domains in the S-layer protein CbsA of Lactobacillus crispatus involved in adherence to collagens, laminin and lipoteichoic acids and in self-assembly, Mol. Microbiol. 46 (2002) 381–394.
[45] J.B. Kaper, V. Sperandio, Bacterial cell-to-cell signaling in the gastrointestinal tract, Infect. Immun. 73 (2005) 3197–3209.